



HAL
open science

Lost in Aggregation: The Local Environmental and Welfare Effects of Large Industrial Shutdowns

Philipp Bothe

► **To cite this version:**

Philipp Bothe. Lost in Aggregation: The Local Environmental and Welfare Effects of Large Industrial Shutdowns. 2024. halshs-04753523

HAL Id: halshs-04753523

<https://shs.hal.science/halshs-04753523v1>

Preprint submitted on 25 Oct 2024

HAL is a multi-disciplinary open access archive for the deposit and dissemination of scientific research documents, whether they are published or not. The documents may come from teaching and research institutions in France or abroad, or from public or private research centers.

L'archive ouverte pluridisciplinaire **HAL**, est destinée au dépôt et à la diffusion de documents scientifiques de niveau recherche, publiés ou non, émanant des établissements d'enseignement et de recherche français ou étrangers, des laboratoires publics ou privés.

LOST IN AGGREGATION: THE LOCAL ENVIRONMENTAL AND WELFARE EFFECTS OF LARGE INDUSTRIAL SHUTDOWNS

PHILIPP BOTHE

WORKING PAPER N°2024/22

OCTOBER 2024

WORLD
INEQUALITY
..... LAB

Lost in Aggregation: The Local Environmental and Welfare Effects of Large Industrial Shutdowns

Philipp Bothe*

October 2024

Abstract

The clean energy transition and large-scale deindustrialization have caused major changes in the industrial landscape of many high-income economies. This paper investigates how closures of large industrial facilities in Germany affect surrounding communities. By exploiting quasi-random variation in the timing of facility shutdowns, I analyze the neighborhood-level effects of these closures using data at the 1km x 1km grid cell level. I find that shutdowns of industrial sites lead to significant improvements in environmental amenities as represented by air quality. These environmental benefits, however, do not capitalize into increasing housing prices. Instead, housing values fall by up to 5% following facility shutdowns – a result that contrasts with existing evidence for the US context. Neighborhoods affected by industrial closures also experience substantial local downturns with average household income dropping by 4% in the most affected neighborhoods. The resulting total annual income loss attributable to facility shutdowns amounts to €0.7 - €1.9 billion. Using a simplified model of neighborhood choice, I further show that neighborhoods surrounding a closed industrial site become less amenable over time. These findings have important implications for place-based policies in the context of significant structural change. Additionally, using the newly assembled granular data, I reveal biases originating from the ecological fallacy in previous assessments of environmental inequality in Germany and show that there exists significant inequality in the exposure to fine particulate matter across the income distribution.

JEL Codes: D31, L60, Q51, Q52, Q53, R23

Keywords: Air Pollution, Amenities, Environmental Inequality, Plant Closure

*Paris School of Economics & World Inequality Lab, philipp.bothe@psemail.eu. This work was funded by a French government subsidy managed by the Agence Nationale de la Recherche (ANR) under the framework of the "Investissements d'avenir programme" reference ANR-17-EURE-001 and by the European Union under WISE Horizons Grant No 101095219.

The transition to a decarbonized economy and the expansion of renewable energy generation have sparked local economic booms and job creation in many places. At the same time, such large-scale structural change entails disruptions in regions with large employment shares in traditional, carbon intensive industries. The question of who will be the winners and losers of the clean energy transition has triggered heated discussions in many high-income economies. While employment in renewable energy has increased almost fourfold since the beginning of the century in Germany ([Umweltbundesamt, 2020](#)), structural change has heavily affected certain regions and contributed to increasing wage inequality ([Goebel and Gornig, 2015](#)). In this light, the question of what happens to neighborhoods that experience shutdowns of major industrial sites naturally arises. This paper constructs a novel dataset at the 1km x 1km grid cell level to shed new light on this question.

In a first step, I quantify the current degree of inequality in terms of access to environmental amenities as measured by air quality and proximity to industrial sites. This exercise reveals a significant degree of inequality in Germany. Low-income neighborhoods face an annual *PM2.5* exposure burden that is $0.5 \mu\text{g}/\text{m}^3$ higher than that of more affluent neighborhoods - a gap that amounts to 0.22 standard deviations of pollution exposure across the full period. Similarly, neighborhoods from the bottom of the income distribution are significantly more likely to be located within direct proximity of a large industrial site than grid cells from the top of the income distribution. These facts have been overlooked in previous studies of environmental inequality in Germany which are conducted at more aggregate levels.

Building on the granular data, I exploit the staggered closure of large industrial sites in Germany to causally estimate the effect of these closures on environmental quality and socio-economic conditions at the neighborhood level. The estimates show that, while shutting down industrial sites improves local air quality, the most affected neighborhoods lose 4% in disposable household income annually relative to the period before the closure. The total annual loss in income incurred by these neighborhoods amounts to €0.7 - €1.9 billion. Similarly, housing prices drop by 5% four years after the shutdown in neighborhoods surrounding closed industrial sites. This finding indicates that the positive environmental amenity effect of improved air quality does not capitalize into increased housing prices but is outweighed by local economic downturns - a result that contrasts with existing findings from the US.

Lastly, I use a revealed preferences approach to quantify the overall amenity impacts from large industrial closures. My findings show that neighborhoods that experience facility closures in their vicinity become slightly less amenable over time. This effect is observed despite improvements in air quality which should in principle make the affected places more amenable. Hence, these neighborhoods face an interacting double burden on welfare - decreasing income and deteriorating amenities follow the shutdown of major industrial sites. These findings make a case for targeted compensation and place-based policy in the most affected neighborhoods to counteract phenomena of persistent regional deprivation observed in other countries.

1 Background

What is the role of local environmental amenities in shaping the residential and economic composition of communities? This question has received considerable attention among environmental and urban economists over the past decades. Seminal contributions illustrate the importance of environmental quality in shaping the composition of modern cities and communities (Banzhaf and Walsh, 2008; Currie et al., 2015; Hebllich et al., 2021). In many cases, however, environmental quality correlates with other amenities and local employment opportunities. For instance, in a place where a large industrial site induces a significant environmental disamenity but also provides employment to the local population, the local net welfare effects of shutting down such a site are unclear. Against the backdrop of ongoing deindustrialization and the phase-out of nuclear and coal power, there are various communities in Germany that are facing such trade-offs.

The US-centered literature has produced exhaustive evidence on the distributional implications of the clean energy transition (Carley and Konisky, 2020), regional decline in coal communities (Colmer et al., 2024; Krause, 2023), and the neighborhood effects of exogenous changes in local environmental quality (Banzhaf and Walsh, 2008; Chay and Greenstone, 2005; Currie et al., 2015; Gamper-Rabindran and Timmins, 2011; Zivin and Singer, 2022). At the same time, the literature is significantly less conclusive regarding the local impacts of the renewable energy transition and structural change in Europe. Recent contributions suggest significant worker-level costs of the coal transition in the UK and Germany (Haywood et al., 2024; Rud et al., 2024). I contribute to the emerging literature for Europe by combining novel data on the closure of large industrial sites in Germany with socio-economic data at the small spatial scale. This paper relates to two major strands of the literature. The descriptive part of the paper contributes to the rapidly growing field of environmental justice research while the second part interests itself in the local-level effects of large industrial shutdowns.

Regarding the first strand, ever since the seminal report of Chavis and Lee (1987) exposed striking racial and socio-economic injustices with respect to the location of hazardous waste sites among US communities, researchers have devoted considerable attention to the empirical and theoretical study of environmental amenities and their distribution. A first part of the

literature is chiefly concerned with quantifying the exposure to environmental disamenities across different ethnic and socio-economic groups.

In this context, persuasive evidence showing that non-white and economically deprived communities are exposed to disproportionate environmental burdens for a variety of pollutants has been put forward (see e.g. [Ash and Boyce, 2018](#); [Bell and Ebisu, 2012](#); [Miranda et al., 2011](#); [Mohai et al., 2009](#)). Inequality in exposure to ambient air pollution has been one of the most salient research areas in this regard ([Mohai et al., 2009](#); [Pais et al., 2014](#)). Recent studies appear to find some reductions in fine particulate matter exposure disparities. [Currie et al. \(2020\)](#) attribute a narrowing of the racial PM_{2.5} exposure gap to over proportionate air quality improvements in predominantly black neighborhoods induced by the Clean Air Act. [Colmer et al. \(2020\)](#) find a convergence effect between the most and least polluted census tracts in the US over the period 1981-2016 albeit strong persistence in relative exposure disparities.

A second strand of the literature has investigated the effects of changing environmental amenities on a variety of socio-economic and demographic outcomes at varying geographical levels. [Banzhaf and Walsh \(2008\)](#) were among the early studies to document residential sorting in response to pollution from TRI sites in the US. [Currie et al. \(2015\)](#) show that housing prices decrease in the immediate proximity of newly opened TRI sites illustrating the potentially significant effects of local environmental amenities on neighborhood-level outcomes. [Gamper-Rabindran and Timmins \(2011\)](#) provide evidence for environmental gentrification, i.e. increased household income and shares of college-educated population within a neighborhood following the cleanup of toxic waste sites. Such evidence on the importance of environmental quality for mechanisms of residential sorting has led to the inclusion of environmental amenities in quantitative spatial models which can rationalise location decisions on the basis of location-specific amenities among other variables ([Bayer et al., 2016](#); [Heblich et al., 2021](#)). More recently, ([Graff Zivin and Singer, 2022](#)) show that, on top of unequal base amenities, there exist significant differences in amenity capitalization rates across racial groups when environmental quality does improve. Their results show that the same air quality improvement translates into stronger housing price increases for white households relative to non-white households in the US because white households are more likely to benefit from capitalization gains through favorable correlated amenities in their neighborhoods. In sum-

mary, there exists a body of evidence on the role of environmental amenities in determining neighborhood composition largely focussed on the anglo-saxon context.

As for Germany, [Bauer et al. \(2017\)](#) show that the decision to close nuclear power plants led to an average decrease in housing prices of 5% along with significant employment reductions in the immediate proximity of closed plants. These results imply that the detrimental economic effects of plant shutdowns dominate the positive amenity effect of reduced nuclear risk perception. In a recent contribution, [Quentel \(2023\)](#) shows that housing prices in Germany also decrease by approximately 2% in reaction to the proximate construction of new wind farms. As wind farms construction should not have any significant local employment effects, this estimate is likely to represent a pure amenity effect driven by factors such as noise pollution or visual disamenities. [Haywood et al. \(2024\)](#) further show significant worker-level welfare costs for German coal miners following the phase-out of coal mining in Germany.

In light of the existing literature, the contribution of this paper is twofold: I first quantify the current state of environmental inequality in Germany with regard to air pollution and proximity to industrial sites at the grid cell level - an exercise that has not been conducted at a reasonable level of spatial disaggregation in a longitudinal setup. Secondly, I exploit quasi-random variation in the closure of large industrial sites to estimate the neighborhood-level impacts of these shutdowns - which, in many cases, represent a simultaneous shift in environmental quality and economic conditions.

2 Data

The analysis in this paper relies on the combination of data from five main sources: remote sensing data on air pollution and weather variables, real estate and socio-economic data for the contiguous area of Germany on grid cell level and information on industrial facilities and their location. The data is annual and spans a common period from 2009 to 2021 at the level of $1km \times 1km$ grid cells. This section describes the individual datasets which have been combined to construct the database used in the analysis.

2.1 Socio-Economic Data

Socio-economic data at the grid cell level are obtained from the *Leibiz Institute for Economic Research (RWI)*. The data is provided on a regular grid with more than 300,000 grid cells across the country. Retaining only populated cells results in a panel of approximately 220,000 grid cells of $1km^2$ covering all populated areas of Germany. The grid is based on the EU-INSPIRE projection whose aim is to facilitate a harmonised provision of spatial information. The data was made available by the RWI as scientific use file where observations are censored if less than five household live within a grid cell ([RWI and Microm, 2023](#)). The dataset is constructed based on more than 1 billion individual observations from a variety of sources, including official statistics, data from private geomarketing companies and data collected by public enterprises such as the *Deutsche Post* ([Breidenbach and Eilers, 2018](#)). The data is validated using official statistics and observations from the Socio-Economic Panel (SOEP), the largest household panel in Germany which includes detailed information on household location.

The dataset contains information on the residential structure of the grid cells, demographic information on population, age structure, share of foreign-born residents and economic variables such as unemployment and disposable household income. I complement the grid cell data with information on the industrial employment share at the district level from the German *Federal Institute for Research on Building, Urban Affairs and Spatial Development (BBSR, 2024)*. Precisely, the industrial employment share is measured as the share of employees in industrial employment in the total working age population.

2.2 Real Estate Data

Real estate data is also retrieved from the research data center at the *RWI*. The data is constructed from listings on Germany's largest online real estate platform *ImmobilienScout24* and contains monthly observations on the number of listings, mean and median rental rates and sale prices for houses and apartments respectively for the period from 2007 to 2022. The data is provided on the same grid as the socio-economic variables. I thus aggregate the real estate data to the annual level and match it with the socio-economic information for the common period of 2009 to 2021.

It is important to note that the data is based on the listings of one single platform only. A priori, there is no way to ensure that the properties listed on this platform are representative of the real estate market in all regions of Germany. As landlords and sellers are required to pay a fee to post their offers on the website, it may be that the propensity to use the platform is higher for relatively more expensive properties. In this case, the observed prices would not be representative of the overall real estate market in Germany. While this is a valid concern, *ImmobilienScout24* is the largest platform for real estate listings in Germany with a market share of approximately 70% of all rental and sale offerings combined in 2016. Given that most properties are offered on multiple platforms at the same time, such a large market share does plausibly imply that most online real estate listings in Germany do appear on *ImmobilienScout24*. Furthermore, the platform is equally used by private home owners and professional real estate agents which are likely to represent different market segments.

Another concern is that the prices indicated in the dataset represent offering prices only. Hence, I do not observe the final sales or rental prices of the different properties. This is arguably a more severe issue for sales than for rentals as there is likely a larger margin of negotiation for property sales than for rental leases. This is potentially problematic if the difference between offer price and final sale price varies systematically across regions as a function of the local real estate market. While such regional variation in the relative difference between listing and final sales price might exist, it appears unlikely to be large enough to invalidate the listing price as a good proxy for the final sale price.

2.3 Air Pollution Data

Pollution Data for ambient ground-level mean $PM_{2.5}$ concentration stems from estimates provided by the Atmospheric Composition and Analysis Group (ACAG) at Washington University.¹ The surface $PM_{2.5}$ estimates are based on a combination of several data sources, most importantly data from ground-based monitoring networks and data on aerosol optical depth based on satellite imagery.² Direct measurements of surface concentration are naturally the most reliable source of pollution data. However, they are usually exclusively located in urban areas and monitoring networks are extremely sparse in many countries and rural areas in particular. [van Donkelaar et al. \(2016\)](#) therefore combine the monitoring data with information on aerosol optical depth (AOD) based on satellite imagery. AOD is a measure of the extent to which aerosols prevent the reflection of light from the earth's surface to the top of the atmosphere and is thus directly related to the volume of aerosols in a given column of air ([Wei et al., 2020](#)). AOD measurements are available at fine spatial resolutions thanks to satellite remote sensing. [van Donkelaar et al. \(2016\)](#) use AOD data projected onto a $0.01^\circ \times 0.01^\circ$ grid covering the entire globe. While AOD is a general measure of the density of particles of a given size in a column of air between the surface of the earth and the atmosphere, it can be related to specific pollutants, such as $PM_{2.5}$ through a model of atmospheric chemistry. [van Donkelaar et al. \(2016\)](#) make use of GEOS-Chem, a geochemical transport model to derive a relationship between the general AOD data and $PM_{2.5}$ pollution levels at the grid cell level.³ These geophysical estimates are then validated against the observed ground-level measurements from monitoring stations. The resulting pollution estimates are available at a resolution of $0.01^\circ \times 0.01^\circ$ which corresponds to grid cells of just over 1 km^2 at the equator. [Fowle et al. \(2019\)](#) show that remote sensing data on $PM_{2.5}$ exhibit considerable attenuation bias and tend to underestimate extreme pollution concentrations. Their results show significant attenuation at pollution concentrations of $15 \mu\text{g}/\text{m}^3$ and above. While such concentrations do occur in Germany, they are present only within the upper end of the pollution distribution. Nonetheless, it is important to keep in mind that exposure at the higher end of the pollution

¹Data is available at: <https://sites.wustl.edu/acag/datasets/surface-pm2-5/> (Accessed 29.11.2021)

²The data for European measurement stations can be retrieved from the EEA's Air Quality e-Reporting database available at: <https://www.eea.europa.eu/data-and-maps/data/aqereporting-9>

³The model is open source and publicly available at: <http://www.geos-chem.org>

distribution might be underestimated.

Since the air pollution data and the socio-economic data are provided roughly at the same resolution, I compute average annual grid cell PM_{2.5} exposure as the area-weighted mean of the pollution grid cells that overlap with a given reference grid cell. Figure A.1 shows the spatial distribution of PM_{2.5} at the grid cell level for Germany at the start and end of the sample period respectively.

2.4 Weather Data

In order to control for variation in annual weather patterns, I obtain data on mean monthly precipitation and temperature on a $0.5^\circ \times 0.5^\circ$ grid from the *Climate Research Unit at the University of East Anglia* (Harris et al., 2020). I further use data on wind speed and direction at the same spatial resolution from the ERA5 global reanalysis dataset (Hersbach et al., 2020). I aggregate the data to the annual level and merge it to the reference grid for Germany provided by the *RWI*.

2.5 Industrial Facility Data

Finally, I retrieve data on polluting industrial facilities in Germany from the EU Industrial Reporting Database.⁴ This database results from the integration of two previously existing sources, namely the European Pollutant Release and Transfer Register (E-PRTR) and the data reported under the EU Industrial Emission Directive (IED) (European Environment Agency, 2023).⁵ Both of these EU directives regulate the reporting of industrial activities and the associated emissions and are applied at the level of industrial facilities. The key difference between the two separate reporting requirements lies in the scope of the activities that are regulated. IED reporting is more focused on monitoring emissions, compliance with emission limit values, and permit conditions for specific industrial activities covered by the directive.

⁴I use the 2023 release of the data (version 8) available at <https://www.eea.europa.eu/data-and-maps/data/industrial-reporting-under-the-industrial-7/eu-registry-e-prtr-lcp>.

⁵The respective legislation for reporting under the IED and the E-PRTR can be found at <https://eur-lex.europa.eu/eli/dir/2010/75/oj> and <https://eur-lex.europa.eu/legal-content/GA/TXT/?uri=celex:32006R0166>

On the other hand, E-PRTR reporting is broader and includes a wider array of industrial sectors, focusing specifically on the release and transfer of pollutants to the environment, irrespective of whether they fall under the IED.⁶

Given that many industrial facilities meet the reporting requirements of both, the IED and the E-PRTR, the Industrial Reporting Database now combines the data which is reported under the two directives. This does not imply that the legislation itself has been changed, the reporting requirements have remained unchanged for both directives, only the resulting data is now reported under a common infrastructure. The latest version of the Industrial Reporting Database covers 99,500 industrial facilities in the EU, 13,318 of which are located in Germany.

The combined database contains information on the location of the regulated facilities, their parent companies, the main industrial activities of the facilities and the type and amount of all released pollutants that fall under the regulation requirements. The data also documents which medium pollutants are released into (air, water or soil). A drawback of the previous reporting databases, in particular the E-PRTR, was that facilities could drop out of the reporting if the releases of specific pollutants dropped below the respective reporting thresholds for these pollutants. More precisely, the E-PRTR regulation defines reporting requirements based on two criteria (i) the physical size of the facility installations (e.g. the burning capacity of a waste incinerator) and (ii) pollutant-specific reporting thresholds (e.g. the amount of NO_x released in a given reporting year). This implies that facilities whose installation size is below the reporting thresholds can drop out of the reporting if their emissions of the specific pollutant which made them eligible for reporting falls below the threshold. In this case, the facility would not be observed in the data in the year where the pollutant threshold is not exceeded and there would be no way of inferring whether this was due to fluctuations in emission levels around the reporting threshold or due to the closure of the respective facility. This caveat is overcome in the new database as closed facilities remain in the database and facility status is reported as one of "operating", "disused", "decommissioned" or "notRegulated", thus enabling me to distinguish between facilities that stop operating and those who stop reporting their emissions because they have dropped below respective reporting thresh-

⁶The specific reporting requirements are documented in Annex I of the corresponding directives cited above.

olds. This feature of the data currently only records the status for non-functional sites after 2016.

I match the facility data with the grid cell information by projecting the coordinates of facility location onto the reference grid for the socio-economic data. I assign a facility to a grid cell if the area of the grid cell overlaps with a buffer of radius r around the point coordinates for the facility provided in the Industrial Reporting Database. Using a radius of five km around the point coordinates of the facilities, there exist 118,000 grid cells that are located within proximity of an operating facility at some point during the sample period. Furthermore, there are 509 distinct facilities in the data whose status changes from "functional" to either "disused" or "decommissioned" at some point during the observation period. This translates to approximately 17,400 grid cells within a 5km radius of facilities that change their status from "functional" to "decommissioned" or "disused" at some point during the sample period. For these grid cell I can directly infer that there is at least one large industrial facility in their proximity that stops operating during the observed period. Figure [A.7](#) plots the location of these grid cells throughout Germany.

The combination of the above sources results in a dataset of roughly 2,000,000 grid cell - year observations for the common period 2009-2021. Note that the socio-economic data is available starting in 2005 and the air pollution and weather data are available at even longer horizons. Therefore, in the parts of the paper that do not rely on the IRD or real estate data, I use the full available time period starting in 2005.

3 PM2.5 Exposure Across the Income Distribution

Before investigating the effects of industrial shutdowns on local welfare, it is useful to quantify the current state of environmental justice with respect to air pollution in Germany. In this regard, the following section is devoted to a descriptive exploration of these patterns at the small spatial scale.

While the US-centered literature has produced a wealth of evidence on unequal pollution exposure at varying levels of aggregation, many existing papers on the link between socio-

economic variables and environmental hazards in the European context face one of two problems. Either, their unit of analysis is some relatively large predefined administrative unit, which typically masks a significant degree of within-unit variation in the socio-economic variable of interest (e.g. household income) and makes them susceptible to issues related to the ecological fallacy (Banzhaf et al., 2019), or, when the analyses are conducted at a more disaggregated level, they typically draw on cross-sectional data (see e.g. Neier, 2021; Rüttenauer, 2018), thereby making any comparison over time impossible.⁷ Figure A.2 illustrates the aggregation problem by plotting the distribution of PM2.5 exposure across pollution and income percentiles respectively within the city of Berlin in 2021. The figure shows that there is considerable variation within Berlin – variation that would be aggregated into one municipality if the analysis were to be conducted at this level.⁸

Figure A.2 illustrates how using aggregate data overlooks a considerable degree of within-unit variation in pollution exposure. This can lead to spurious conclusions with regard to inequality in pollution exposure. It is thus natural to ask how the PM2.5 exposure gradient across the income distribution changes when moving from municipality-level to more granular data. I investigate this by regressing the mean annual PM2.5 concentration on an indicator variable for the income decile that a given grid cell belongs to in a model of the following form

$$PM_{2.5,nt} = \sum_{k=2}^{10} \theta_k \times 1[D_{nt} = k] + X_{nt} \delta' + C_{nt} \beta' + \omega_{l \times t} + \varepsilon_{nt} \quad (1)$$

where $PM_{2.5,nt}$ denotes the mean annual concentration of PM2.5 in grid cell n in year t , D_{it} indicates which national-level income decile grid cell n belongs to in year t , X_{nt} and C_{nt} are vectors of socio-economic and meteorological controls respectively.⁹ Finally, $\omega_{l \times t}$ is a vector of land-by-year fixed effects which capture regional shocks at the *Bundesländer* level, the

⁷Examples of studies conducted at a higher level of spatial aggregation include European Environmental Agency (2018); Germani et al. (2014); Lavaine (2015); Richardson et al. (2013) and a meta-study for Europe has been conducted by Fairburn et al. (2019).

⁸Hsiang et al. (2019) further show that the cross-sectional relationship between household income and exposure to air pollution in the US is highly sensitive to the administrative level it is estimated at.

⁹The meteorological controls contain average temperature and precipitation at the grid cell level.

highest administrative unit below the federal level in Germany. This choice is motivated by the relatively high degree of administrative and political autonomy of the *Bundesländer*, enabling them to enact policies that might influence pollution concentrations differently across different *Bundesländer* and independently from federal legislation.

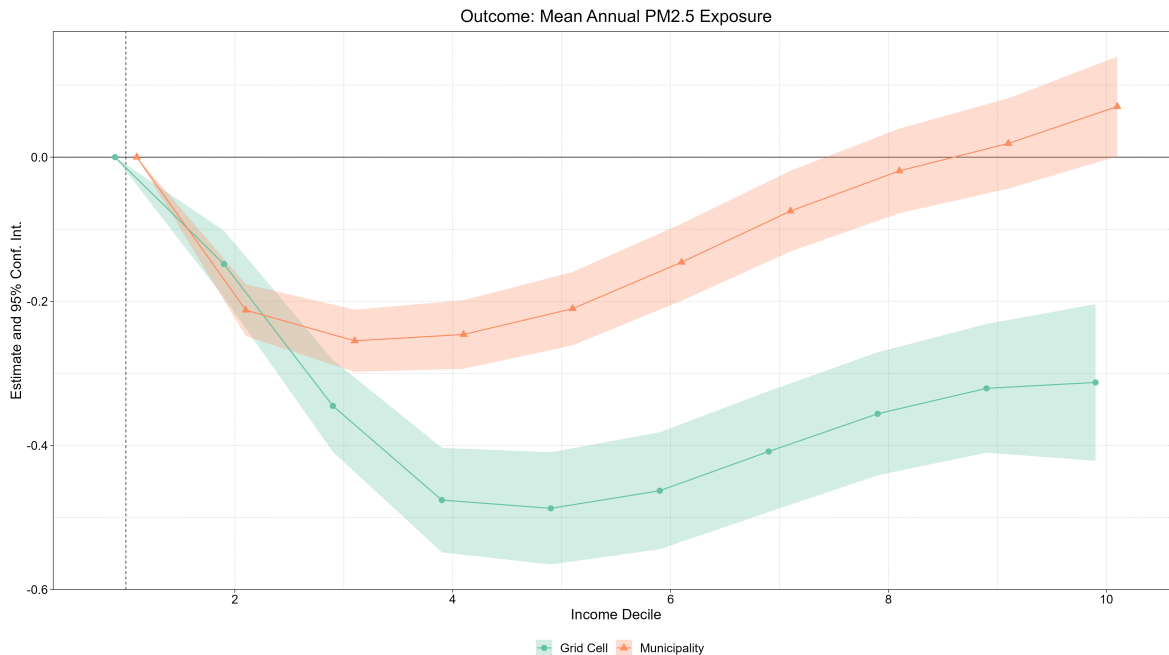
Figure A.5 illustrates the results from this exercise using a model with and without grid cell fixed effects. The results show that when comparing all grid cells across Germany, there exists a large and significant gap in PM_{2.5} exposure between the most modest and the more affluent neighborhoods in Germany. The suggestive U-shaped pattern is consistent with some existing cross-sectional evidence on exposure disparities and may be explained by higher pollution concentrations in comparatively more affluent urban agglomerations (Champalaune, 2020; Hsiang et al., 2019). Such regional differences (along with other constant grid cell features) are absorbed in the specification using grid cell fixed effects. Nonetheless, the empirical fact that the bottom 20% of the income distribution face significantly higher pollution loads than higher income neighborhoods persists when estimated using only within-grid cell variation.

Additionally, it is noteworthy that the results in Figure A.5 are obtained while controlling for the share of foreign born residents per grid cell. Hence, income remains a significant predictor of pollution exposure in Germany even when controlling for a proxy of ethnicity. This is a notable results as it contrasts with existing studies which suggest that race is the predominant predictor of environmental injustice and income plays a subordinate role when race/ethnicity is accounted for (see e.g. Hernandez-Cortes et al., 2023; Neier, 2021; Rüttenauer, 2018).

To compare these results to analyses conducted at the level of administrative units, I aggregate the grid cell data to the municipality level and reestimate Equation 1 at the municipality level. Figure 1 compares the estimates obtained at the two levels of aggregation. The findings indicate that analyses of environmental justice conducted at the municipality level in Germany suffer from ecological fallacy biases. While the grid cell analysis shows a significant exposure gap between the bottom and the top of the income distribution, the model estimated at municipality level does not suggest a difference in pollution burden between the bottom 10% and the top 30% of the income distribution. This result clearly illustrates how the use of aggregate data can lead to spurious conclusions with regard to environmental justice and

underlines the importance of granular data to quantify exposure differentials.

Figure 1: Cross-Sectional Ambient PM_{2.5} Exposure Across the Income Distribution



Note: The graph displays point estimates and 95% confidence intervals for β_k from Equation (1) estimated at the level of grid cells (dots) and municipalities (triangles) without unit fixed effects. The omitted decile in both models is the bottom decile. Estimates represent exposure differentials relative to the bottom decile.

The above results suggest that low-income neighborhoods see themselves exposed to significantly higher levels of harmful ambient air pollution than their more affluent counterparts. Such differences in mean exposure are likely to correlate with increased occurrence of extreme pollution loads. This fact is illustrated by Figure A.3 which shows the population share of each income decile within the top pollution decile for each year. The graph shows that the poor bear a disproportionate exposure burden when it comes to extreme pollution levels (i.e. those above the 90th percentile of the pollution distribution). The poorest 30% of grid cells account for more than 50% of the population in the most polluted regions throughout almost the entire sample period. At the same time, relatively more affluent neighborhoods are clearly underrepresented within the top pollution decile.¹⁰ The richest grid cells account for

¹⁰Figure A.4 in the Appendix shows the same graph for pollution exposure around the median for comparison.

population shares far below 5% for most of the observed period. This disproportionate share of low-income grid cells within the top of the pollution distribution is still observed in recent years despite a reduction in absolute pollution levels. The average share of the richest neighborhoods among the most polluted places in Germany is equal to 4.3% compared to 19.6% for the neighborhoods from the lowest income decile. Hence, while the absolute pollution burden has been decreasing in Germany in recent years, the exposure distribution remains skewed and low-income areas continue to be exposed to the highest observed pollution levels in the country at a much higher likelihood than richer areas. Given that the concentration of PM_{2.5} exceeds WHO health guidelines virtually everywhere in Germany, this exposure gradient is likely to directly translate into an unequal distribution of the detrimental effects associated with exposure to fine particulate matter.

In summary, although purely descriptive so far, the empirical results show a clear pattern of environmental inequality with respect to air pollution exposure in Germany - the degree of which is significantly more pronounced than one would find in aggregate municipality-level data. Hence, economic deprivation and exposure to ambient air pollution tend to coincide at the neighborhood level. In this light, it is pertinent to ask how shocks to local amenities influence the relative welfare of neighborhoods. Answering this question is the aim of the subsequent sections.

4 The Impact of Large Industrial Shutdowns

What role do industrial sources play in shaping the overall distribution of exposure to fine particulate matter? While traffic is one of the main sources of fine particulate matter, industrial sources such as power plants, steel production or livestock farming are significant contributors to the overall pollution load. The European Environment Agency (EEA) estimates that air pollution from industrial facilities alone caused damages of up to €50 billion in 2017. These damage estimates are cumulated across all air pollutants and damage types, such as damages to human health, productivity or agriculture and are contingent on specific parameter choices (regarding the VSL, for instance). Nonetheless, these estimates illustrate the relevance of air pollution from industrial sources for the overall pollution burden. Similarly, seminal papers such as [Currie et al. \(2015\)](#) show the detrimental effect of industrial facility presence on public health. It is thus straightforward to see the environmental disamenity effect that comes with the presence of industrial sites and existing studies have found evidence for residential segregation in response to the presence of industrial sites ([Gamper-Rabindran and Timmins, 2013](#)). This section provides new evidence on the causal effect of industrial shutdowns on both, environmental and economic outcomes in surrounding neighborhoods.

To begin with, it is useful to establish whether there exists a correlation between the location of IRD sites and neighborhood income in Germany.¹¹ To this end, [Figure A.6](#) in the Appendix plots the share of grid cells within the direct proximity (i.e. located within the focal or a directly adjacent grid cell) of an operating IRD site as a function of the within-district income percentile pooled across all observation years. The graph shows that within a district, poorer grid cells have a significantly higher propensity of being located close to polluting industrial sites.

Hence, all else equal, industrial shutdowns might be beneficial from an environmental justice standpoint as they are likely to increase environmental quality in comparatively low-income

¹¹There is a large body of work on the correlation between neighborhood characteristics and proximity to pollution sources (see e.g. [Ash and Boyce, 2018](#); [Rüttenauer, 2018](#)) These studies have raised questions around the drivers of inequality in pollution exposure. Explanations that have been evoked are residential sorting, i.e. 'coming to the nuisance' dynamics, selective siting of polluting firms into deprived areas, etc.. Here, I do not attempt to explain the drivers of the observed correlation

neighborhoods. However, when such industrial sites are also a main provider of employment options to the local community, the presumed improvement in environmental quality may be outweighed by other impacts on local outcomes so that the sign of the net welfare effect is not clear a priori. The following section is thus devoted to disentangling the welfare effects of shutting down large industrial sites.

4.1 Empirical Strategy

I am interested in causally estimating the neighborhood level impact of shutting down IRD sites on several outcomes of interest. To this end, I exploit the staggered treatment adoption (i.e. variation in shutdown timing across different locations) to estimate an event study model of the following form

$$Y_{nt} = \sum_{s \neq -1} \theta_s \times 1[Closure_{nt}] \times 1[t - \tau_n = s] + \mathbf{C}_{nt}\beta' + \alpha_n + \omega_{l \times t} + \varepsilon_{nt} \quad (2)$$

where $Closure_{nt}$ is an indicator variable that equals one if grid cell n is within a 5km radius of a facility that stops operating in year t , τ_n is the year of first treatment for grid cell n and all remaining variables are as defined above. I define grid cell n as treated if at least one facility in its vicinity is shut down, even when other operating IRD facilities are present. For grid cells that are located within the intersection of multiple treatment buffers, i.e. such grid cells that are within a 5km radius of multiple facilities, I consider a grid cell as treated once the first facility in its vicinity has been shut down. Since the binary treatment status does not change again once a given grid cell has moved into the treated group, this implies that some grid cells receive additional treatment doses while already being considered as treated. Figure A.7 maps all the places in Germany that experience such a closure during the sample period. I estimate Equation (2) on the subsample of grid cells that experience a closure at some point during the sample period. This reduces the sample used to estimate the causal effects of facility shutdown to approximately 220,000 grid cell – year observations. Using only observations that will eventually experience a closure implies that there are no *never treated* units in the sample and the control group for treated units are *not yet treated* grid cells, i.e. those grid cells for which $\tau_n > t$ in a given year t . As compared to the commonly used con-

control buffer approach, this approach has the advantage of avoiding potentially "contaminated" comparisons between treated and presumably untreated units within a control buffer with larger radius around the treatment buffer. Aside from the arbitrariness of choosing treatment and control buffer radii, the control buffer approach has been shown to suffer from SUTVA violations due to spillover effects. It further requires strong assumptions for identification of a direct treatment effect (Pollmann, 2023). By using *not yet treated* grid cells as control units, the identifying assumption in the above model becomes that the timing of facility closures across units is quasi-random and does not structurally depend on any unobserved grid cell characteristics. I bin all pre-treatment years that precede the closure by five years or more into one category. I further restrict the endpoint of the event window to four years after treatment adoption to avoid biases that may arise due to the decreasing size of the control group.

4.2 Air Quality Impacts

In order to get an empirical hold on the different impacts of industrial shutdowns, the first step is to establish whether there exists a statistically significant link between the presence of industrial facilities and the concentration of fine particulate matter. The average effect of shutting down an IRD site on PM_{2.5} concentration in surrounding neighborhoods across all post-treatment periods is displayed in the first row of Table 1. The effects are statistically significant and consistent across all specifications. On average, shutting down one IRD site reduces annual PM_{2.5} concentration in surrounding neighborhoods by approximately $0.2\mu\text{g}/\text{m}^3$ - an effect that corresponds to 0.12 standard deviations of PM_{2.5} concentration at baseline. To further corroborate these results and show that the observed pollution reductions are attributable to the industrial shutdown, the second row displays results for the same model where the treatment variable is interacted with an indicator for whether grid cell n is located downwind relative to the treatment plant it is assigned to. A grid cell is considered downwind in year t if it is located within the half-circle obtained by bisecting the treatment buffer along a line perpendicular to the predominant wind direction computed at the level of the municipality the facility is located in. Again, the results are statistically significant and of constant magnitude across all models. The estimated dynamic effects of facility closures on

air pollution concentration in surrounding grid cells are shown in Figure A.8.¹²

Table 1: Effect of Facility Shutdown on PM2.5 Concentration in Surrounding Neighborhoods

Dependent Variable:	PM2.5		
Model:	(1)	(2)	(3)
Closure	-0.1856*** (0.0546)	-0.1909*** (0.0523)	-0.1990*** (0.0525)
Closure \times Downwind	-0.2141*** (0.0643)	-0.2157*** (0.0600)	-0.2221*** (0.0598)
<i>Fixed Effects</i>			
Grid Cell	Yes	Yes	Yes
Bundesland \times Year	Yes	Yes	
Year			Yes
Weather Controls		Yes	Yes
Mean (SD) at t-1	11.30 (1.72)		
Observations	223,801	223,801	223,801

Standard errors clustered by municipality
*Signif. Codes: ***: 0.01, **: 0.05, *: 0.1*

Note: The first row shows point estimates and standard errors for the treatment effect of facility shutdowns on surrounding grid cells as defined in Equation 2 averaged across all post-treatment periods. The second row reports results from the same model where treatment is interacted with an indicator variable for whether a given grid cell n is located downwind from the closest industrial site to be shut down during the observation period.

The results clearly indicate that shutting down IRD facilities induces a positive effect on air quality. Four years after the shutdown, mean annual PM2.5 exposure is reduced by 0.48 $\mu\text{g}/\text{m}^3$ on average. Interestingly, while there appears to be an immediate pollution reduction following the shutdown, the air quality improvement builds up during the years following the shutdown. This could either be driven by an overall reduction in industrial activity and related traffic that follows the closure of a major industrial hub within a local network or by the fact that, given the way treatment is defined, grid cells that are in the intersection of two or more treatment buffers receive an additional treatment dose from further shutdowns in their

¹²I estimate Equation (2) using the two-stage estimator proposed in Gardner et al. (2024) via the accompanying R command *did2s* to account for potential treatment effect heterogeneity across treatment adoption dates.

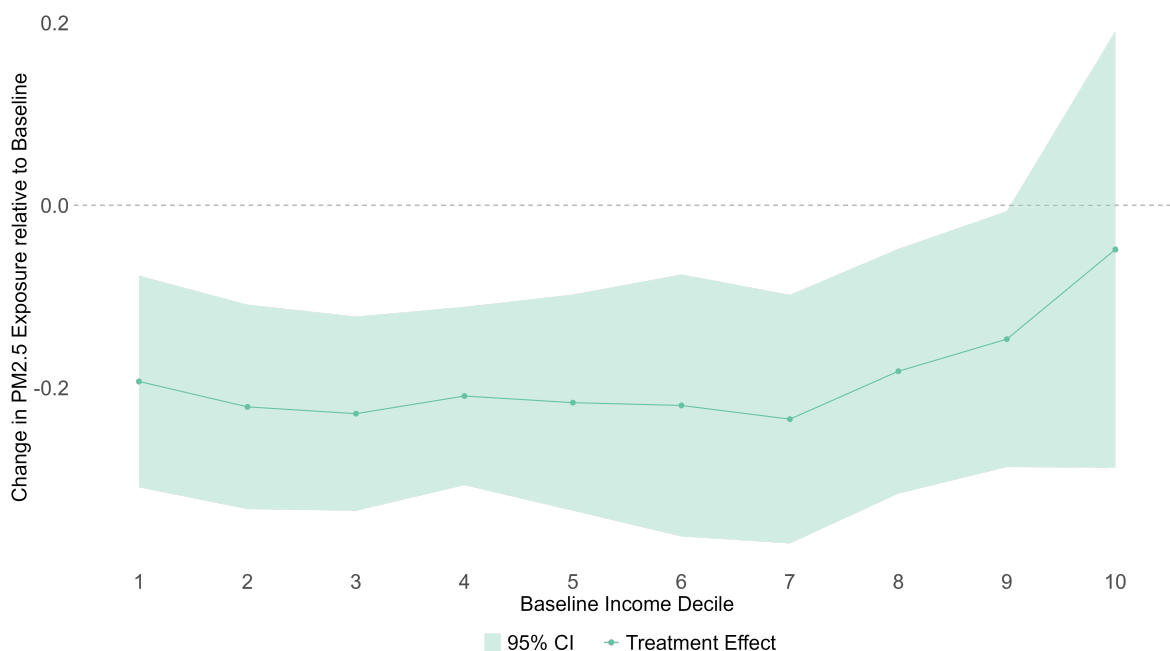
proximity while already in the treated group.

In summary, the results show clear local air quality improvements following the shutdowns of IRD sites. Further, it is noteworthy that, given the size of the treatment buffer, the estimated effect on air quality is entirely attributable to avoided primary PM_{2.5} release at the emission source and does not include presumably large additional benefits from reductions in secondary PM_{2.5} which can be realised at large distances from the emission source.

4.3 The Effect of Industrial Shutdowns on the PM_{2.5} Exposure Gap

The estimates displayed in Table 1 represent the average effect of shutting down IRD sites on air quality in surrounding neighborhoods. To assess the impact of these shutdowns on the degree of inequality in pollution exposure, Figure 2 plots the treatment effect from the specification used in column (2) of Table 1 separately for each income decile. The results indicate that air quality improvements from IRD shutdowns are fairly uniform for neighborhoods from the bottom 70% of the income distribution while comparatively high-income grid cells benefit less from air quality improvements induced by facility shutdowns. Hence, IRD shutdowns contribute to narrowing the gap in pollution exposure between the most deprived and the most affluent neighborhoods at the local level. A priori, the effect on the national level pollution gap cannot be evaluated based on these estimates as such an evaluation would require information on the dispersion of air pollutants from the closing plants across the entire area of Germany before shutdown. While modern chemical transport models are capable of providing such estimates in principle, such an exercise is outside the scope of this paper.

Figure 2: Treatment Effect Heterogeneity for PM2.5 by Income Decile



Note: The figure shows the average treatment effect and 95% confidence interval of facility shutdowns on PM2.5 concentration in surrounding neighborhoods averaged across all post-treatment periods by baseline income decile of the treated grid cells. Estimates correspond to results obtained using the model in Column (2) of Table 1 with treatment interacted with baseline income decile.

4.4 The Local Economic Consequences of Industrial Closures

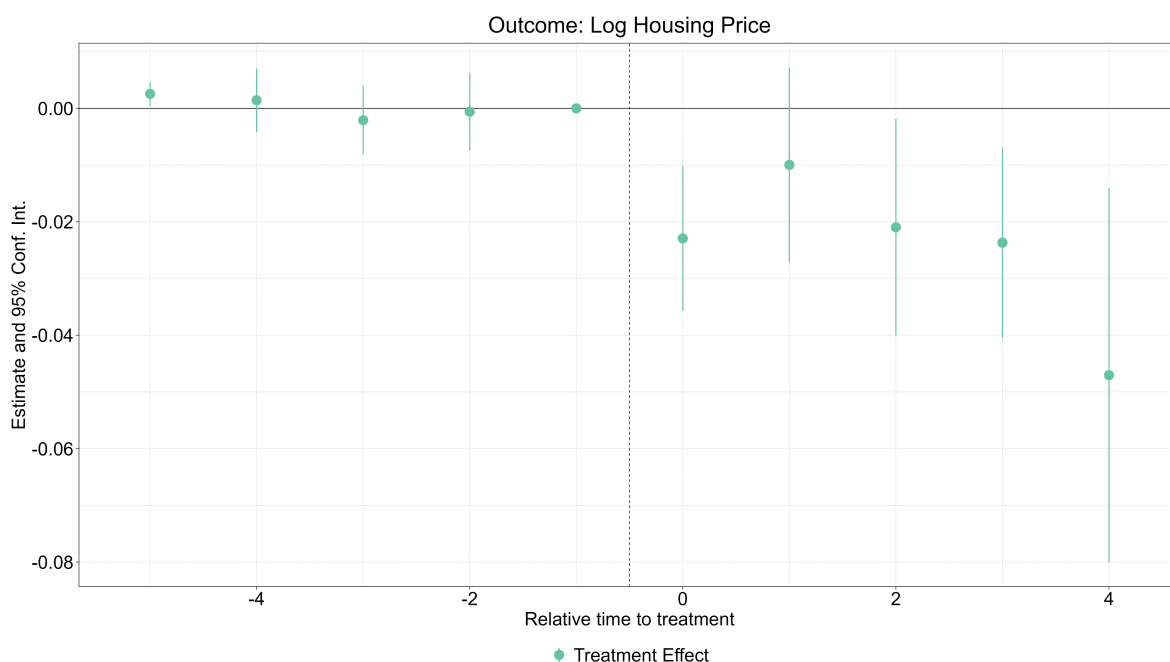
Figure A.8 shows that industrial closures cause significant improvements in local air quality - shutting down large IRD sites thus arguably represents a positive environmental amenity shock. At the same time, IRD plants represent large industrial sites that can play a major role within local economies. Hence, the local welfare impacts of shutting down such sites depend on more factors than the improvement in environmental quality. Regarding the US context, [Gamper-Rabindran and Timmins \(2013\)](#) provide evidence for increases in neighborhood level income following TRI closures which might plausibly be driven by environmental gentrification mechanisms. Similarly, [Fraenkel et al. \(2022\)](#) show increases in housing prices following decreased local pollution from coal power plants. These estimates would suggest that a decrease of industrial pollution is followed by a revaluation of the surrounding neigh-

borhoods in terms of residential attractiveness. To assess whether these results translate to the European context, I reestimate Equation (2) with a variety of economic outcome variables.

To begin with, I quantify the impact of IRD shutdowns on average housing price per square meter (in logs) of house and apartment sales at the neighborhood level. I restrict the sample to neighborhoods in which at least 5 house or apartment sales are recorded in the data in a given year. Figure 3 displays the effect of facility closures on the average housing price in grid cells within a 5km radius around the closed facilities. The estimates show a significant drop in housing prices starting immediately after the shutdown. By year $t+4$, the decrease in housing prices reaches 5% relative to the pre-shutdown period. Hence, housing prices substantially drop following IRD closures despite the significant improvements in local air quality. This finding suggests that the positive environmental amenity effect of increased air quality is outweighed by other detrimental effects on the valuation of neighborhoods surrounding a closed plant. Interestingly, these results contrast with the US literature which finds either no effect of plant closures on housing prices (Currie et al., 2015) or positive capitalization effects of coal plant unit retirements (Fraenkel et al., 2022) or general pollution improvements (Chay and Greenstone, 2005; Zivin and Singer, 2022). It thus appears that the local "cleanup effect" induced by shutting down large industrial sites does not capitalize into housing values in Germany.

The negative effect of facility closures on housing prices suggests that the improvements in environmental amenities are not represented in the hedonic valuation of these neighborhoods. However, it is important to bear in mind that (i) in the presence of effects on population composition, the housing price estimates cannot be interpreted as WTP for facility shutdowns and (ii) the housing price estimates represent the net effect of multiple changes to the environmental and economic conditions of the neighborhoods that occur simultaneously. It may thus be that the air quality improvements *are* valued but do not appear as positive price effects because they are outweighed by the detrimental local economic shocks induced by plant closures. This interpretation is in line with the results by Bauer et al. (2017) who find significant housing price declines in the vicinity of closed nuclear power plants in the wake of the Fukushima accident in Germany.

Figure 3: Effect of facility closures on log housing price in surrounding grid cells



Note: The figure shows point estimates and 95% confidence intervals for θ_s in Equation 2. The outcome variable is average log housing price per square meter at the grid cell level for grid cells with at least five house or apartment sales per year. The model is estimated without controls. The full sample consists of all grid cells within a 5km radius around plants that close down during the sample period. Standard errors are clustered by *Bundesland*. All estimates are weighted by grid cell population.

Therefore, to assess whether industrial shutdowns induce significant local economic downturns, I finally also estimate Equation (2) using neighborhood level employment and mean annual disposable household income as outcome variables. As for the employment effect, shutting down IRD facilities significantly drives up neighborhood unemployment starting two years after the shutdown. Four years after the closure, average unemployment is 0.3 percentage points higher than before the shutdown (see column (3) in Table A.3). Relative to a mean unemployment rate of 6.97% at baseline, the rise in unemployment following IRD shutdown appears relatively mild.

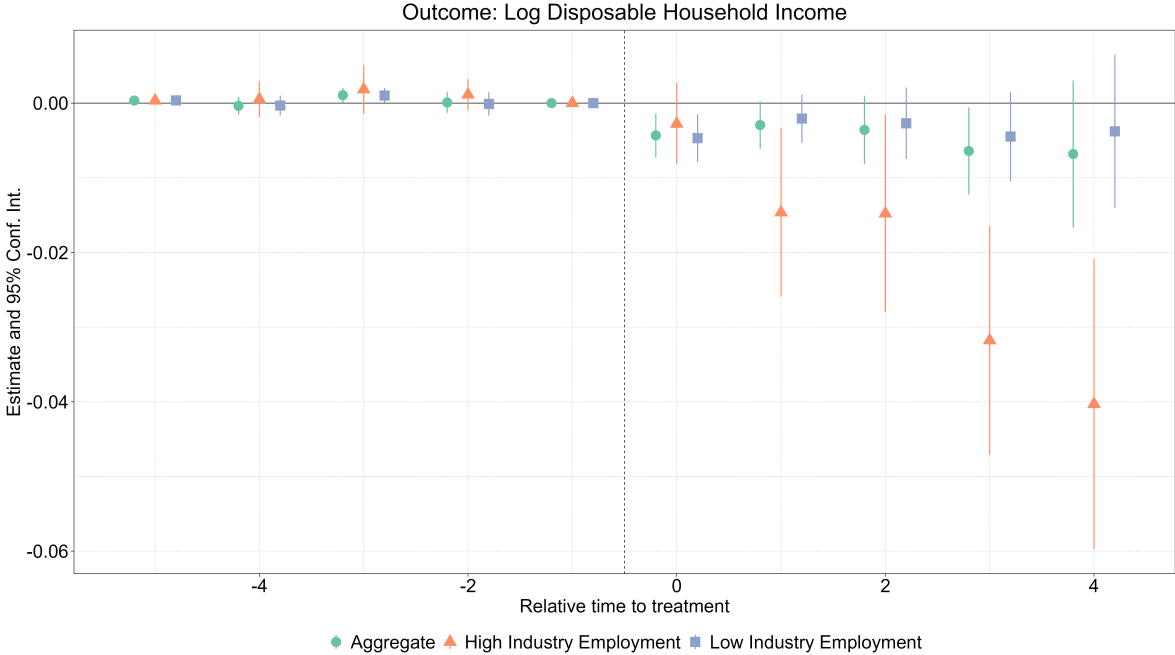
Regarding the effects on neighborhood income, the estimates plotted in Figure 4 show that, at the aggregate, there appears to be no significant effect on average neighborhood income from

facility closures. This result might be driven by neighborhoods where industrial employment does not play a significant role in overall employment. I thus estimate the model separately for two subgroups of neighborhoods: grid cells that are located within districts with an industrial employment share above and below 25%, respectively (results are also reported in Figure 4). The results expose significant heterogeneity with respect to the income effects induced by industrial closures. The estimates show that, while areas with comparatively low industrial employment shares do not face significant income shocks following industrial closures, neighborhoods with significant industrial employment do experience significant losses in average household income. These effects reach up to 4% of lost disposable household income annually four years after a shutdown. Interestingly, this effect is robust to controlling for neighborhood level unemployment (see Figure A.11). Hence, the observed income losses do not predominantly originate from prolonged unemployment but presumably represent the effect of switching to lower skilled or part-time employment following the industrial shutdown. This finding is in line with Haywood et al. (2024) who show that the largest fraction of welfare losses experienced by coal miners in the clean energy transition in Germany is explained by switching to lower paid employment rather than persistent unemployment.

Table A.2 in the Appendix displays the unconditional absolute income effects of facility shutdowns by baseline industrial employment. Neighborhoods located within districts with high baseline industrial employment share see their mean income drop by an average amount of €930 four years after the closure - an effect equivalent to approximately 0.2 standard deviations of baseline income in the complete estimation sample. Based on these estimates, it is possible to perform a simple back-of-the-envelope calculation to estimate the total annual amount of foregone income attributable to facility closures. In total, roughly 2,700 grid cells are located in districts with baseline industrial employment above 25% and experience a shutdown during the sample period. Figure A.10 displays the location of these grid cells. These neighborhoods have an average adult population of 525 inhabitants per grid cell. Hence, the total adult population within the subsample of neighborhoods that exhibit significant income losses amounts to just over 1.4 million adults. Based on the 95% confidence interval for the estimated coefficient four years after shutdown, the total income loss falls within the range of €0.7 to €1.9 billion - an amount equal to between 0.2 and 0.4% of total federal public

expenditure in Germany in 2023.

Figure 4: Effect of Facility Closures on Disposable Household Income per adult (in logs)



Note: The figure shows point estimates and 95% confidence intervals for θ_s in Equation 2. The outcome variable is log disposable household income per adult at the grid cell level. The model is estimated without controls. The dots represent the aggregate effect in the full sample, triangles represent estimates for grid cells located in districts with industrial employment share equal to or above 25%, squares represent estimates for grid cells located in districts with industrial employment shares below 25%. The full sample consists of all grid cells within a 5km radius around plants that close down during the sample period. Standard errors are clustered by *Bundesland*. All estimates are weighted by grid cell population.

4.5 Estimating the Net Amenity Effects of Industrial Closures

The results so far indicate that facility closures simultaneously entail significant air quality gains and detrimental local economic effects in a relevant subset of neighborhoods. The negative housing price effects appear to indicate that the economic losses outweigh the environmental gains in terms of welfare impacts. However, if the neighborhoods affected by industrial shutdowns experienced substantial amenity improvements, then these could potentially compensate the income losses in welfare terms. Therefore, the following section lays out a framework that allows for the estimation of the net amenity effects of industrial closures. The model used in this section builds on the canonical Rosen-Roback framework (Rosen, 1974; Roback, 1982) and is directly adapted from Bartik et al. (2019) who in turn build on the seminal work by Moretti (2011). Quentel (2023) provides a recent application of the framework for the German context.

Consider an economy that consists of N neighborhoods denoted by n and is populated by a mass of L workers denoted by l . Location-specific individual utility is a function of neighborhood amenities (A_n), the consumption of housing (h) and a numéraire consumption good (c) and a location-specific taste shock (θ_{ln}). Let the price of housing and the wage rate in neighborhood n p_n and w_n respectively. Assuming that workers' utility is Cobb-Douglas and that every worker inelastically supplies one unit of labor in the neighborhood they live in, the workers' maximization problem writes as

$$\begin{aligned} \max_{c,h} u_{ln} &= A_n \cdot h^\alpha \cdot c^{1-\alpha} \cdot \theta_{ln} \\ \text{s.t. } h \cdot p_n + c &= w_n. \end{aligned} \tag{3}$$

The solution to the above problem yields the indirect utility of living in neighborhood n .¹³

¹³Since the utility takes a standard Cobb-Douglas form, the solution to the consumer problem is straightforward. The full derivation is given in the appendix.

$$U_{ln} = \frac{A_n w_n}{p_n^\alpha} \theta_{ln} \quad (4)$$

Hence, the probability that a worker chooses neighborhood n over any neighborhood r is given by

$$\mathbb{P}\left(\frac{A_n w_n}{p_n^\alpha} \theta_{nl} \geq \frac{A_r w_r}{p_r^\alpha} \theta_{rl}\right) \quad \forall r \neq n.$$

Assuming that the neighborhood specific taste shocks are distributed according to a Type II extreme value distribution with shape parameter ϕ , i.e. $\theta_{ln} \sim F(\theta_n) = \exp(-\theta^{-\phi})$, the share of workers living in neighborhood n is given by

$$s_n = \frac{\left(\frac{A_n w_n}{p_n^\alpha}\right)^\phi}{\sum_{r=1}^N \left(\frac{A_r w_r}{p_r^\alpha}\right)^\phi}. \quad (5)$$

Recall that total population in the economy is equal to L , so that the population in neighborhood n is equal to $R_n = L \cdot s_n$. Substituting into (5) and taking logs of the equation, we can solve for amenities in neighborhood n as a function of observables and amenities in other neighborhoods.

$$\ln(A_n) = \frac{1}{\phi} \ln(R_n) + \alpha \ln(p_n) - \ln(w_n) - \frac{1}{\phi} \ln(L) + \frac{1}{\phi} \ln\left(\sum_{r=1}^N \frac{A_r w_r}{p_r^\alpha}\right)^\phi \quad (6)$$

For estimation purposes, note that the total population L and the sum $\sum_{r=1}^N \frac{A_r w_r}{p_r^\alpha}$ vary across years, but not across grid cells. Hence, introducing a time dimension and subsuming the two terms that are constant in cross-section into c_t , Equation (6) writes as

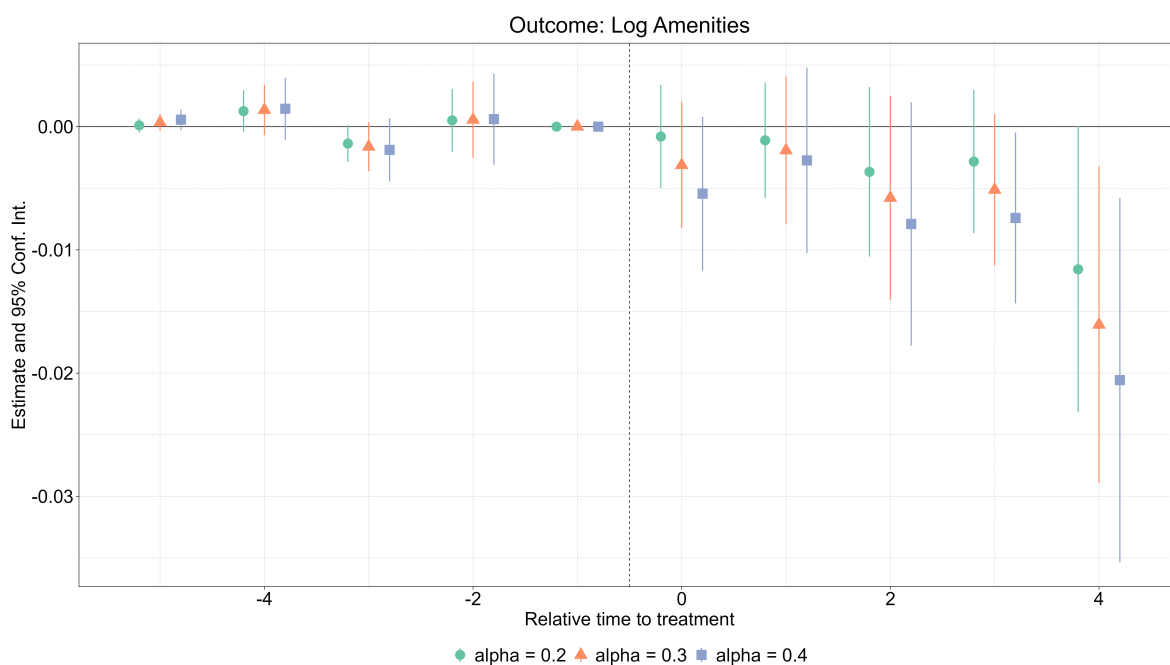
$$\ln(A_{nt}) = \frac{1}{\phi} \ln(R_{nt}) + \alpha \ln(p_{nt}) - \ln(w_{nt}) + c_t \quad (7)$$

Under the assumption that average disposable income per grid cell is a reasonable proxy for wages, Equation (7) gives a representation of amenities as a function of observed variables, a time-variant term that will be absorbed by the fixed effects in the empirical application and the parameters ϕ and α . The shape parameter ϕ governs the dispersion of the taste shock. A larger value for ϕ increases the mass in the tail of the probability density function of the taste shock distribution and thus increases the probability that a worker chooses a neighborhood n although it is dominated by another neighborhood with respect to observable characteristics. I follow recent estimates for Germany as provided in [Krebs and Pflüger \(2023\)](#) and calibrated in [Quentel \(2023\)](#) and set $\phi = 4.56$. As for α , the income share spent on housing, the range of parameters used in the literature varies considerably. In one of the seminal contributions to the quantitative spatial literature, [Monte et al. \(2018\)](#) argue for a comparatively high expenditure share of 0.4. [Quentel \(2023\)](#) estimates an expenditure share closer to 0.2 based on data from the German microcensus. I thus compute amenities for a range of values between 0.2 and 0.4 to assess the robustness of the results to the choice of this parameter. I can thus now use Equation (7) to estimate the effect of facility closures on amenities in the affected neighborhoods using the same event-study methodology as above:

$$\ln(A_{nt}) = \sum_{s \neq -1} \theta_s \times 1[Closure_{nt}] \times 1[t = s] + \alpha_n + \omega_{t \times l} + \varepsilon_{nt}$$

where $\ln(A_{nt})$ is computed as in Equation (7) for values of α between 0.2 and 0.4 and c_t is contained in ω_t . The results for different values of α are shown in [Figure 5](#).

Figure 5: Effect of Facility Closures on Log Amenities



Note: The figure shows point estimates and 95% confidence intervals for θ_s in Equation 2. The outcome variable is log amenities at the grid cell level. Amenities are computed as in Equation 7 for values of α between 0.2 and 0.4. The different estimates represent the effect on amenities computed for varying values of α . The full sample consists of all grid cells within a 5km radius around plants that close down during the sample period. Standard errors are clustered by *Bundesland*. All estimates are weighted by grid cell population.

While the estimates are fairly noisy, the results for higher values of α point towards a negative aggregate amenity effect of plant closures on surrounding neighborhoods. In any case, facility closures do not induce positive net amenity effects through the cleanup of polluted neighborhoods. Despite the air quality improvements which should in principle make neighborhoods more amenable, there appear to be other channels at play that decrease the desirability of the affected neighborhoods. Examples of such channels could be a deterioration of public services as a consequence of decreasing corporate tax revenues at the municipality level or the retirement of other businesses or services that correlate with the presence of large employers. For interpretation, it is helpful to recall the indirect utility function in Equation (4) and to note that amenities and income both enter indirect utility multiplicatively without any exponents. Hence, in terms of welfare effects, a one percent change in amenities is equivalent to a one

percent change in income. Therefore, the estimate based on the expenditure share of housing calculated in [Monte et al. \(2018\)](#) would suggest a welfare loss of almost 2% four years after the closure. Note that this is the welfare loss induced by the decrease in amenities only. Given that some neighborhoods already incur significant income losses due to industrial shutdowns, the reduction in amenities adds an additional burden in terms of welfare loss for the neighborhoods. Combining this finding with the observation that industrial facilities tend to be present in poorer neighborhoods within a district, facility closures aggravate regional inequalities and make low-income neighborhoods within a region less amenable despite presumably desirable benefits for environmental quality. These results have important implications for regional inequality and the political management of large scale structural transformation which will be discussed below.

5 Conclusion

Climate change mitigation policies and the energy transition induce large-scale structural change in countries all around the globe. Policies such as the phase-out of coal power generation are often determined at the national level and their macro-level effects are fairly well understood. At the same time, the local environmental and economic repercussions of such policies have not been explored in detail, especially in Europe. I leverage plausibly exogenous variation in the timing of large industrial shutdowns to estimate the local welfare effects of such closures.

Understanding the localized impacts of industrial closures requires an analysis at the small spatial scale. The first contribution of this paper thus lies in assembling information on socio-economic variables, real estate prices and air quality at the neighborhood level for Germany. A descriptive analysis of this novel dataset shows that inequality in exposure to air pollution is significantly underestimated when using more aggregate data at the municipality level. The results show a clear gradient in *PM2.5* exposure across the income distribution - a result that contrasts with studies for the US where race is the dominant determinant of pollution exposure.

I then build on this novel dataset to causally estimate the effect of industrial shutdowns on

environmental quality and welfare at the neighborhood level. The estimates show that industrial closures significantly increase local air quality. However, these improvements in environmental quality do not capitalize into housing price increases. Instead, housing prices drop by over 5% four years after the closure in surrounding neighborhoods - a result that again contrasts with the US literature where pollution reductions tend to capitalize into housing price increases. These results indicate that industrial shutdowns have detrimental effects on local welfare that presumably outweigh the gains in environmental quality. My findings do indeed suggest that neighborhoods that are located in areas with high baseline industrial employment incur significant and sizeable income losses following plant closures. Four years after the shutdown, average disposable household income in these neighborhoods drops by 4% relative to the year before the closure. Using a stylized model of neighborhood choice, I further show that the net change in neighborhood amenities induced by industrial closures is negative despite improved air quality. This finding implies that, in contrast to the environmental gentrification hypothesis, neighborhoods do not become more amenable in the wake of industrial shutdowns and environmental cleanup. Instead, deteriorating amenities add to the welfare loss induced by industrial shutdowns.

Given that industrial plants are more likely to be located in comparatively low-income neighborhoods within a region, my findings suggest that structural change increases local inequality. The results thus have important implications regarding the management of large-scale transformation policies. My estimates provide guidance for thinking about compensation and place-based policies to cushion the effects of industrial shutdowns in the most affected areas (see e.g. [Hanson, 2023](#)). My findings suggest that compensating income losses from past industrial shutdowns would require expenditures between 0.2% and 0.4% of federal public spending in Germany. Further research will require the use of a full quantitative spatial model to investigate trade-offs in welfare from improvements in environmental quality and the slowdown of local economic activity and to determine the optimal spatial allocation of place-based policies to respond to welfare losses incurred by the most affected neighborhoods.

References

- Ash, M. and Boyce, J. K. (2018). Racial disparities in pollution exposure and employment at US industrial facilities. *Proceedings of the National Academy of Sciences*, 115(42):10636–10641.
- Banzhaf, H. S., Ma, L., and Timmins, C. (2019). Environmental Justice: Establishing Causal Relationships. *Annual Review of Resource Economics*, 11(1):377–398.
- Banzhaf, H. S. and Walsh, R. P. (2008). Do People Vote with Their Feet? An Empirical Test of Tiebout’s Mechanism. *American Economic Review*, 98(3):843–863.
- Bartik, A. W., Currie, J., Greenstone, M., and Knittel, C. R. (2019). The Local Economic and Welfare Consequences of Hydraulic Fracturing. *American Economic Journal: Applied Economics*, 11(4):105–155.
- Bauer, T. K., Braun, S. T., and Kvasnicka, M. (2017). Nuclear power plant closures and local housing values: Evidence from Fukushima and the German housing market. *Journal of Urban Economics*, 99:94–106.
- Bayer, P., McMillan, R., Murphy, A., and Timmins, C. (2016). A Dynamic Model of Demand for Houses and Neighborhoods. *Econometrica*, 84(3):893–942.
- BBSR, Stadt-und Raumforschung, B. f. B. (2024). Laufende Raumbewachtung des BBSR - INKAR. Technical Report 03/2024, Bonn.
- Bell, M. L. and Ebisu, K. (2012). Environmental Inequality in Exposures to Airborne Particulate Matter Components in the United States. *Environmental Health Perspectives*, 120(12):1699–1704.
- Breidenbach, P. and Eilers, L. (2018). RWI-GEO-GRID: Socio-economic data on grid level. *Jahrbücher für Nationalökonomie und Statistik*, 238(6):609–616.
- Carley, S. and Konisky, D. M. (2020). The justice and equity implications of the clean energy transition. *Nature Energy*, 5(8):569–577.

- Champalaune, P. (2020). Inequality in Exposure to Air Pollution in France: Measurement and Impact of a City-Level Public Policy. *PSE Master Thesis*.
- Chavis, B. and Lee, C. (1987). Toxic Wastes and Race in the United States: A National Report on the Racial and Socio-Economic Characteristics of Communities with Hazardous Waste Sites. Technical report, United Church of Christ.
- Chay, K. and Greenstone, M. (2005). Does Air Quality Matter? Evidence from the Housing Market. *Journal of Political Economy*, 113(2):376–424.
- Colmer, J., Hardman, I., Shimshack, J., and Voorheis, J. (2020). Disparities in PM_{2.5} air pollution in the United States. *Science*, 369(6503):575–578.
- Colmer, J., Krause, E., Lyubich, E., and Voorheis, J. (2024). Transitional Costs and the Decline of Coal: Worker-Level Evidence. (Working Paper).
- Currie, J., Davis, L., Greenstone, M., and Walker, R. (2015). Environmental Health Risks and Housing Values: Evidence from 1,600 Toxic Plant Openings and Closings. *American Economic Review*, 105(2):678–709.
- Currie, J., Voorheis, J., and Walker, R. (2020). What Caused Racial Disparities in Particulate Exposure to Fall? New Evidence from the Clean Air Act and Satellite-Based Measures of Air Quality. Technical Report w26659, National Bureau of Economic Research, Cambridge, MA.
- European Environment Agency (2023). Industrial reporting under the Industrial Emission Directive 2010/75/EU and European Pollutant Release and Transfer Register Regulation (EC) No 166/2006 Information on the database structure and use. Version 8.
- European Environmental Agency (2018). Analysis of Air Pollution and Noise and Social Deprivation. *Eionet Report - ETC/ACM 2018/7*.
- Fairburn, J., Schüle, S. A., Dreger, S., Karla Hiltz, L., and Bolte, G. (2019). Social Inequalities in Exposure to Ambient Air Pollution: A Systematic Review in the WHO European Region. *International Journal of Environmental Research and Public Health*, 16(17):3127.

- Fowlie, M., Rubin, E., and Walker, R. (2019). Bringing Satellite-Based Air Quality Estimates Down to Earth. *AEA Papers and Proceedings*, 109:283–288.
- Fraenkel, R., Zivin, J. S. G., and Krumholz, S. (2022). The Coal Transition and Its Implications for Health and Housing Values. Technical Report w30801, National Bureau of Economic Research, Cambridge, MA.
- Gamper-Rabindran, S. and Timmins, C. (2011). Hazardous Waste Cleanup, Neighborhood Gentrification, and Environmental Justice: Evidence from Restricted Access Census Block Data. *American Economic Review*, 101(3):620–624.
- Gamper-Rabindran, S. and Timmins, C. (2013). Does cleanup of hazardous waste sites raise housing values? Evidence of spatially localized benefits. *Journal of Environmental Economics and Management*, 65(3):345–360.
- Gardner, J., Thakral, N., Tô, L. T., and Yap, L. (2024). Two-Stage Differences in Differences. *Working Paper*.
- Germani, A. R., Morone, P., and Testa, G. (2014). Environmental justice and air pollution: A case study on Italian provinces. *Ecological Economics*, 106:69–82.
- Goebel, J. and Gornig, M. (2015). Deindustrialization and the Polarization of Household Incomes: The Example of Urban Agglomerations in Germany. *SSRN Electronic Journal*.
- Graff Zivin, J. S. and Singer, G. (2022). Disparities in Pollution Capitalization Rates: The Role of Direct and Systemic Discrimination. *NBER WORKING PAPER SERIES*, 30814:w30814.
- Hanson, G. (2023). Local Labor Market Impacts of the Energy Transition: Prospects and Policies. Technical Report w30871, National Bureau of Economic Research, Cambridge, MA.
- Harris, I., Osborn, T. J., Jones, P., and Lister, D. (2020). Version 4 of the CRU TS monthly high-resolution gridded multivariate climate dataset. *Scientific Data*, 7(1):109.
- Haywood, L., Janser, M., and Koch, N. (2024). The Welfare Costs of Job Loss and De-

- carbonization: Evidence from Germany's Coal Phaseout. *Journal of the Association of Environmental and Resource Economists*, 11(3):577–611.
- Heblich, S., Trew, A., and Zylberberg, Y. (2021). East-Side Story: Historical Pollution and Persistent Neighborhood Sorting. *Journal of Political Economy*, 129(5):1508–1552.
- Hernandez-Cortes, D., Meng, K. C., and Weber, P. (2023). Decomposing Trends in US Air Pollution Disparities from Electricity. *Environmental and Energy Policy and the Economy*, 4:91–124.
- Hersbach, H., Bell, B., Berrisford, P., Hirahara, S., Horányi, A., Muñoz-Sabater, J., Nicolas, J., Peubey, C., Radu, R., Schepers, D., Simmons, A., Soci, C., Abdalla, S., Abellan, X., Balsamo, G., Bechtold, P., Biavati, G., Bidlot, J., Bonavita, M., De Chiara, G., Dahlgren, P., Dee, D., Diamantakis, M., Dragani, R., Flemming, J., Forbes, R., Fuentes, M., Geer, A., Haimberger, L., Healy, S., Hogan, R. J., Hólm, E., Janisková, M., Keeley, S., Laloyaux, P., Lopez, P., Lupu, C., Radnoti, G., De Rosnay, P., Rozum, I., Vamborg, F., Villaume, S., and Thépaut, J. (2020). The ERA5 global reanalysis. *Quarterly Journal of the Royal Meteorological Society*, 146(730):1999–2049.
- Hsiang, S., Oliva, P., and Walker, R. (2019). The Distribution of Environmental Damages. *Review of Environmental Economics and Policy*, 13(1):83–103.
- Krause, E. (2023). Job Loss, Selective Migration, and the Accumulation of Disadvantage: Evidence from Appalachia's Coal Country. *Working Paper*.
- Krebs, O. and Pflüger, M. (2023). On the road (again): Commuting and local employment elasticities in Germany. *Regional Science and Urban Economics*, 99:103874.
- Lavaine, E. (2015). An Econometric Analysis of Atmospheric Pollution, Environmental Disparities and Mortality Rates. *Environmental and Resource Economics*, 60(2):215–242.
- Miranda, M. L., Edwards, S. E., Keating, M. H., and Paul, C. J. (2011). Making the Environmental Justice Grade: The Relative Burden of Air Pollution Exposure in the United States. *International Journal of Environmental Research and Public Health*, 8(6):1755–1771.

- Mohai, P., Pellow, D., and Roberts, J. T. (2009). Environmental Justice. *Annual Review of Environment and Resources*, 34(1):405–430.
- Monte, F., Redding, S. J., and Rossi-Hansberg, E. (2018). Commuting, Migration, and Local Employment Elasticities. *American Economic Review*, 108(12):3855–3890.
- Moretti, E. (2011). Local Labor Markets. In Ashenfelter, O. and Card, D., editors, *Handbook of Labor Economics*, volume 4 of *Handbook of Labor Economics*, pages 1237–1313. Elsevier. Section: 14.
- Neier, T. (2021). Austrian Air – Just Clean for Locals: A Nationwide Analysis of Environmental Inequality. *Ecological Economics*, 187:107100.
- Pais, J., Crowder, K., and Downey, L. (2014). Unequal Trajectories: Racial and Class Differences in Residential Exposure to Industrial Hazard. *Social Forces*, 92(3):1189–1215.
- Pollmann, M. (2023). Causal Inference for Spatial Treatments. arXiv:2011.00373 [econ, stat].
- Quentel, M. (2023). Gone with the Wind: Renewable Energy Infrastructure, Welfare, and Redistribution. Working Paper. \.
- Richardson, E. A., Pearce, J., Tunstall, H., Mitchell, R., and Shortt, N. K. (2013). Particulate air pollution and health inequalities: a Europe-wide ecological analysis. *International Journal of Health Geographics*, 12(1):34.
- Roback, J. (1982). Wages, Rents, and the Quality of Life. *Journal of Political Economy*, 90(6):1257–1278. Publisher: The University of Chicago Press.
- Rosen, S. (1974). Hedonic Prices and Implicit Markets: Product Differentiation in Pure Competition. *Journal of Political Economy*, 82(1):34–55. Publisher: The University of Chicago Press.
- Rud, J.-P., Simmons, M., Toews, G., and Aragon, F. (2024). Job displacement costs of phasing out coal. *Journal of Public Economics*, 236:105167.

- RWI and Microm (2023). Socio-economic data on grid level - Scientific Use File (wave 13) Sozioökonomische Daten auf Rasterebene - Scientific Use File (Welle 13). Artwork Size: 5.07 GB Pages: 5.07 GB.
- Rüttenauer, T. (2018). Neighbours matter: A nation-wide small-area assessment of environmental inequality in Germany. *Social Science Research*, 70:198–211.
- Umweltbundesamt (2020). Indikator: Beschäftigte im Bereich Erneuerbare Energien. Publisher: Umweltbundesamt.
- van Donkelaar, A., Hammer, M. S., Bindle, L., Brauer, M., Brook, J. R., Garay, M. J., Hsu, N. C., Kalashnikova, O. V., Kahn, R. A., Lee, C., Levy, R. C., Lyapustin, A., Sayer, A. M., and Martin, R. V. (2021). Monthly Global Estimates of Fine Particulate Matter and Their Uncertainty. *Environmental Science & Technology*, 55(22):15287–15300.
- van Donkelaar, A., Martin, R. V., Brauer, M., Hsu, N. C., Kahn, R. A., Levy, R. C., Lyapustin, A., Sayer, A. M., and Winker, D. M. (2016). Global Estimates of Fine Particulate Matter using a Combined Geophysical-Statistical Method with Information from Satellites, Models, and Monitors. *Environmental Science & Technology*, 50(7):3762–3772.
- Wei, X., Chang, N.-B., Bai, K., and Gao, W. (2020). Satellite remote sensing of aerosol optical depth: advances, challenges, and perspectives. *Critical Reviews in Environmental Science and Technology*, 50(16):1640–1725.
- Zivin, J. G. and Singer, G. (2022). Disparities in Pollution Capitalization Rates: The Role of Direct and Systemic Discrimination. NBER Working Paper w30814, National Bureau of Economic Research.

A APPENDIX

A.1 Utility Maximization Problem

The utility maximization problem of a worker in neighborhood n is given in Equation (3):

$$\begin{aligned} \max_{c,h} u_{ln} &= A_n \cdot h^\alpha \cdot c^{1-\alpha} \cdot \theta_{ln} \\ \text{s.t. } h \cdot p_n + c &= w_n. \end{aligned} \tag{8}$$

The Lagrangian then writes

$$\mathcal{L} = A_n \cdot h^\alpha \cdot c^{1-\alpha} \cdot \theta_{ln} + \lambda(w_n - h \cdot p_n - c) \tag{9}$$

and the FOCs are given by

$$\frac{\partial \mathcal{L}}{\partial h} = \alpha A_n \theta_{ln} \left(\frac{c}{h}\right)^{1-\alpha} - \lambda p_n \stackrel{!}{=} 0 \tag{10}$$

$$\frac{\partial \mathcal{L}}{\partial c} = (1-\alpha) A_n \theta_{ln} \left(\frac{h}{c}\right)^\alpha - \lambda \stackrel{!}{=} 0 \tag{11}$$

$$\frac{\partial \mathcal{L}}{\partial \lambda} = w_n - h \cdot p_n - c \stackrel{!}{=} 0. \tag{12}$$

Dividing (10) by (11) and using the constraint yields the well-known expressions for optimal consumption under Cobb-Douglas preferences.

$$c = (1 - \alpha) w_n \quad (13)$$

$$h = \alpha \frac{w_n}{p_n} \quad (14)$$

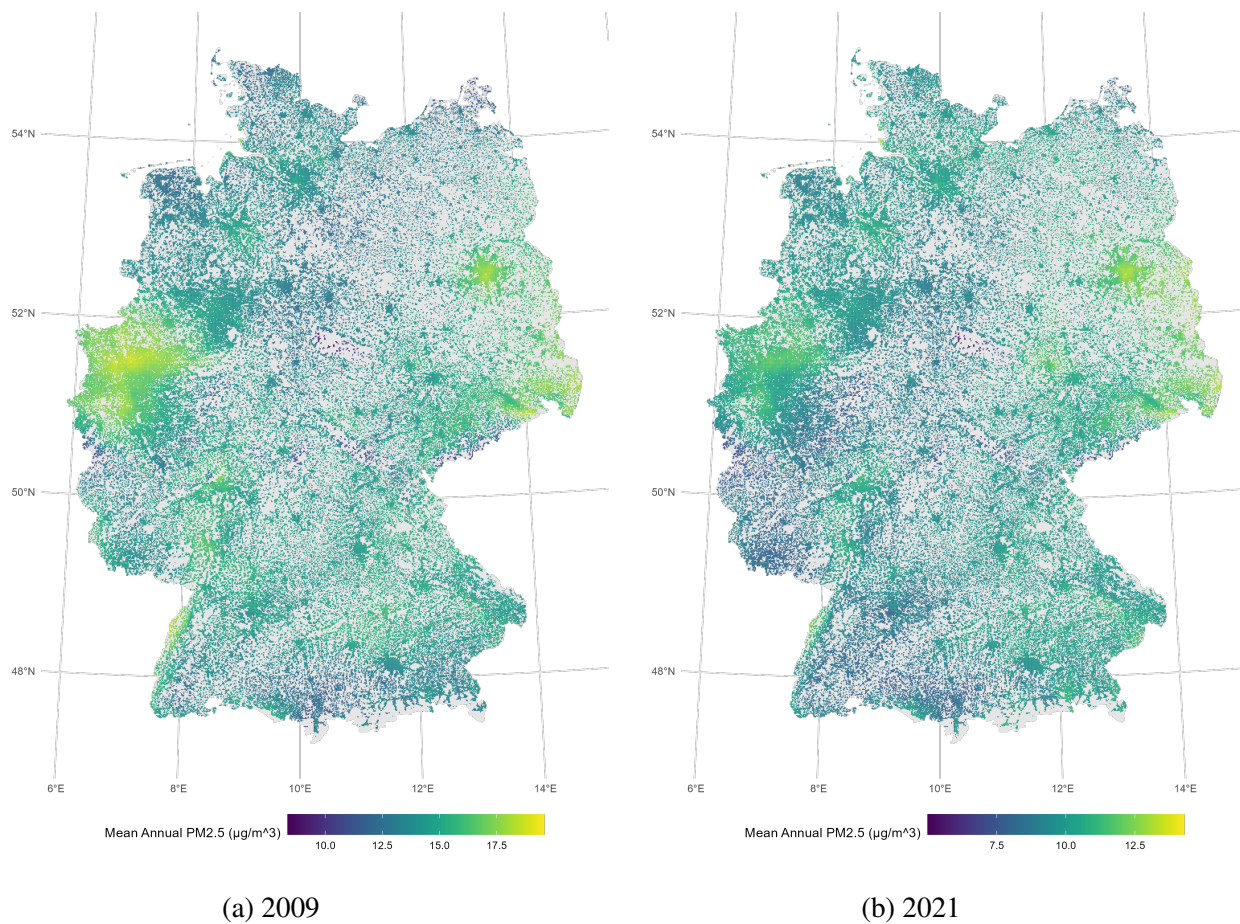
Substituting back into the utility function, we obtain the following expression for indirect utility

$$U_{ln} = \alpha^\alpha (1 - \alpha)^{1-\alpha} \frac{A_n w_n}{p_n^\alpha} \theta_{ln}. \quad (15)$$

Since α is a constant, it can be ignored for ordinal utility comparisons and the expression reduces to Equation (4).

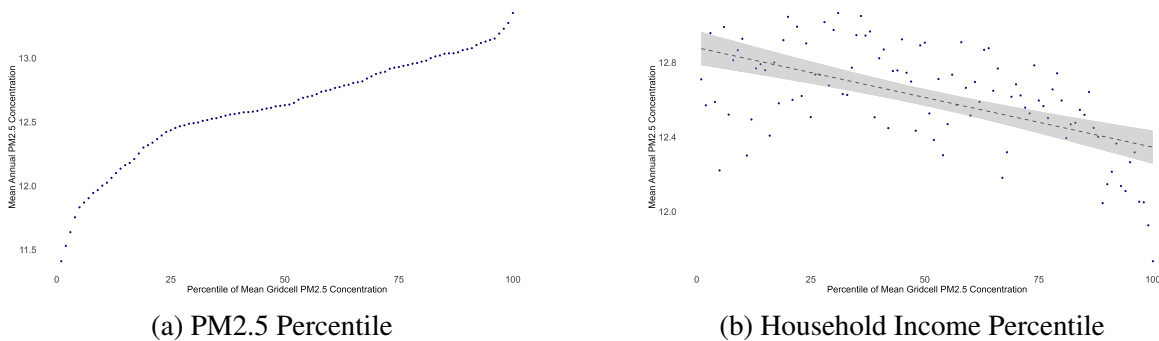
A.2 Figures

Figure A.1: Spatial Distribution of Mean Annual PM_{2.5} Exposure in Germany



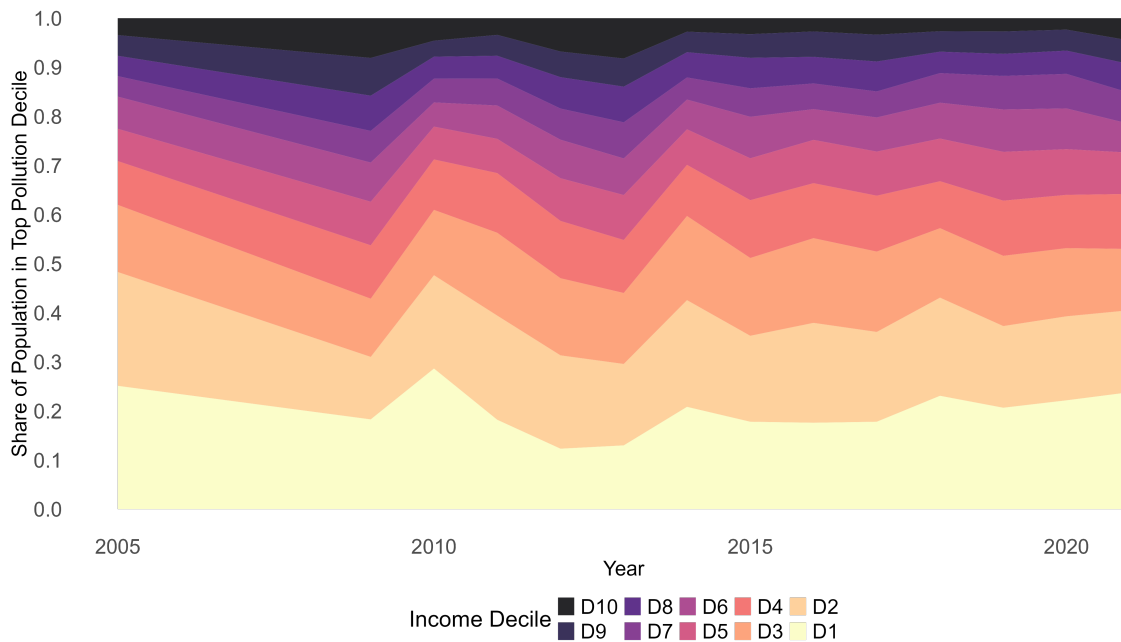
Note: The graph shows the average annual concentration of ambient PM_{2.5} by grid cell in Germany for (a) 2009 and (b) 2021. PM_{2.5} concentration is computed as the area-weighted mean of all pixels from [van Donkelaar et al. \(2021\)](#) that overlap with a given grid cell.

Figure A.2: Within-Municipality Distribution of PM2.5 for Berlin 2021



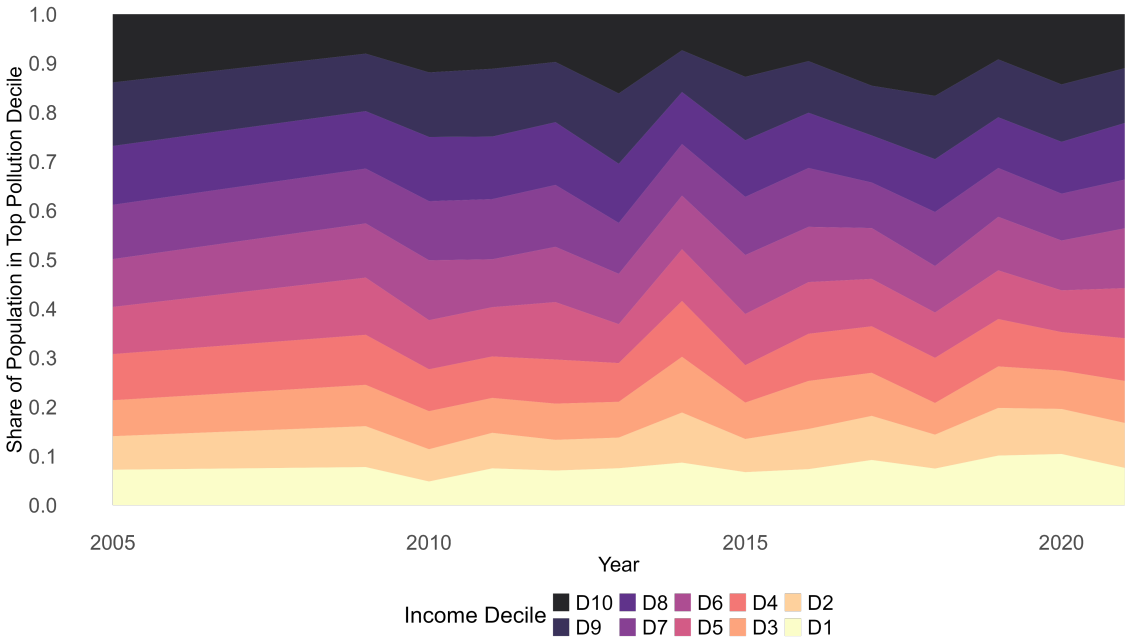
Note: The figure shows the mean PM2.5 exposure across population-weighted percentiles of the pollution distribution (a) and the household income distribution (b) within the municipality of Berlin in 2021. The dashed line in panel (b) represents OLS fit of regressing the mean annual PM2.5 concentration on the household income percentile.

Figure A.3: Share of Population within Top Pollution Decile by Income Deciles, 2009-2021



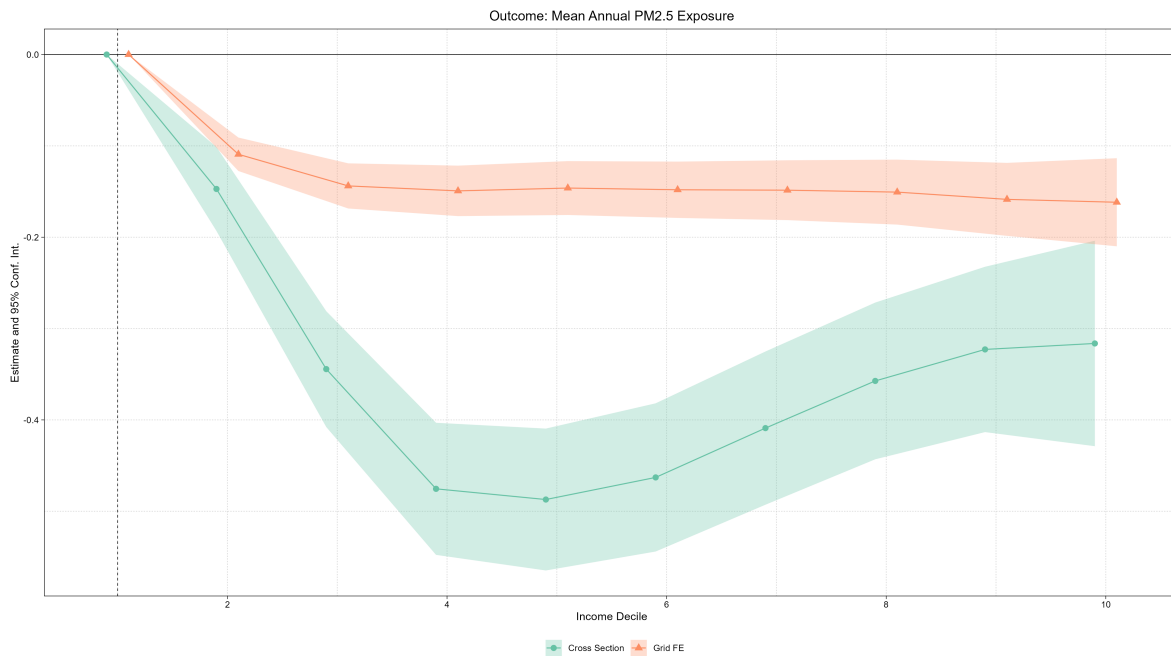
Note: The plot shows the composition of the population within the neighborhoods that belong to the top decile of PM2.5 exposure in Germany by income decile for every year in the sample period. Income deciles are population weighted, so that each decile comprises 10% of the German population instead of 10% of neighborhoods.

Figure A.4: Share of Population in p45p55 of the Pollution Distribution by Income Decile, 2009-2021



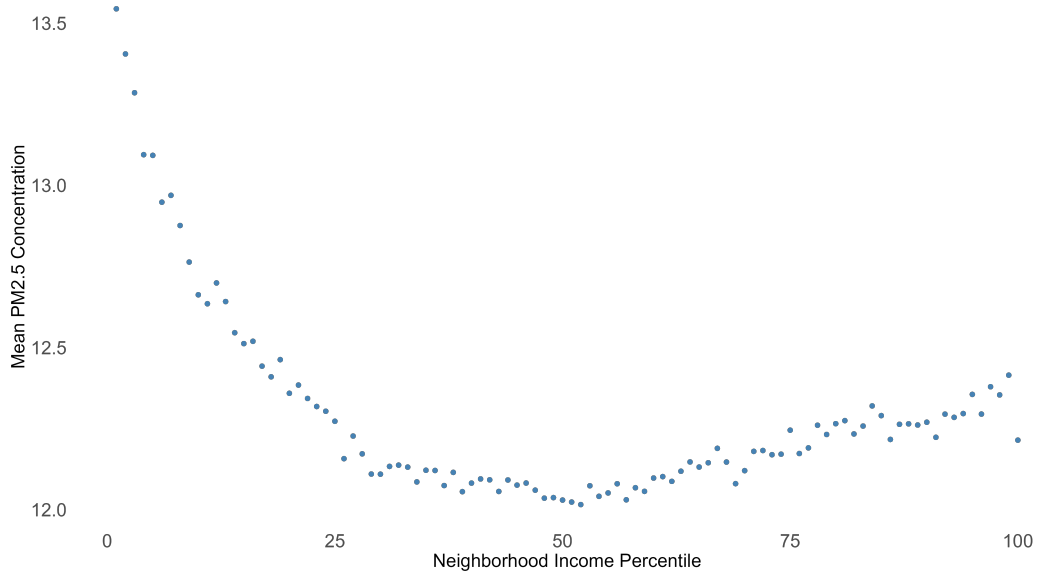
Note: The plot shows the composition of the population within the neighborhoods that are between the 45th and the 55th percentile of PM2.5 exposure in Germany by income decile for every year in the sample period. Income deciles are population weighted, so that each decile comprises 10% of the German population instead of 10% of neighborhoods.

Figure A.5: PM2.5 exposure difference with respect to bottom income decile of grid cells



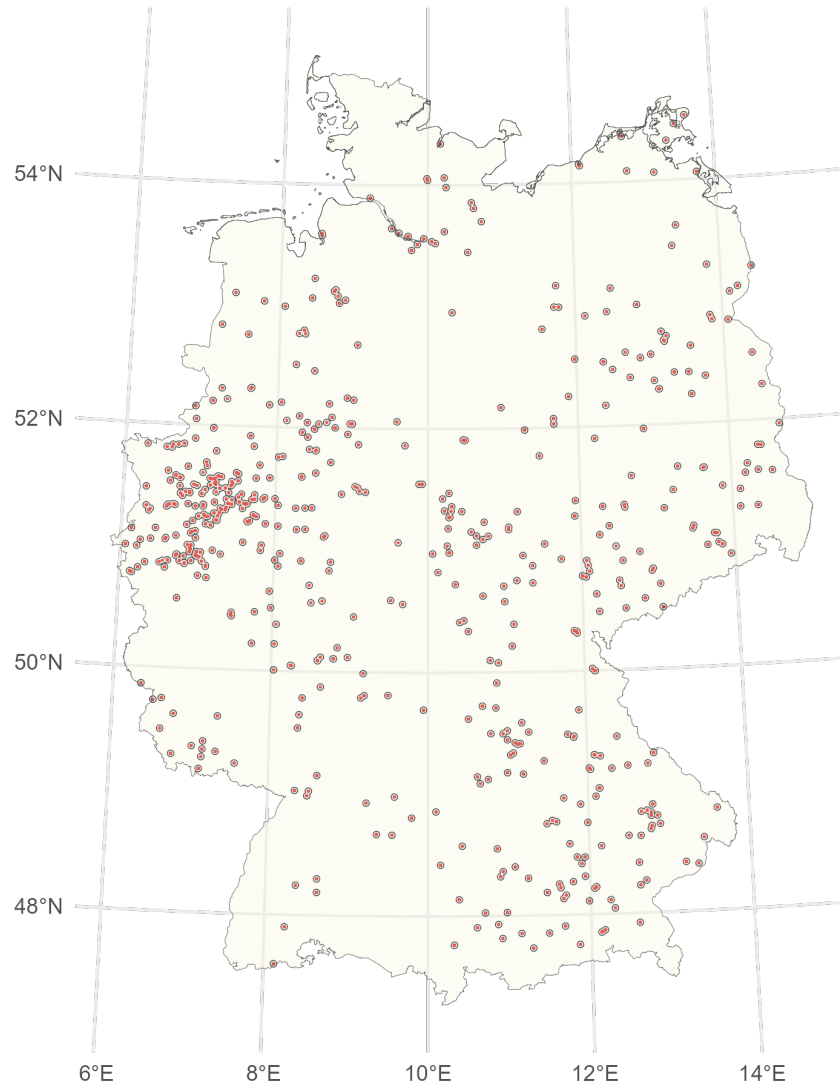
Point estimates and 95% confidence intervals for β_k from Equation (1), with and without grid cell FE Note: The graph displays estimates and 95% confidence intervals for β_k from Equation (1). The estimated effects display PM2.5 exposure relative to the bottom decile. Controls include average annual temperature and precipitation and the share of foreign born residents at the grid cell level. Standard errors are clustered by *Bundesland*.

Figure A.6: Association Between Neighborhood Income and Proximity to IRD Facilities



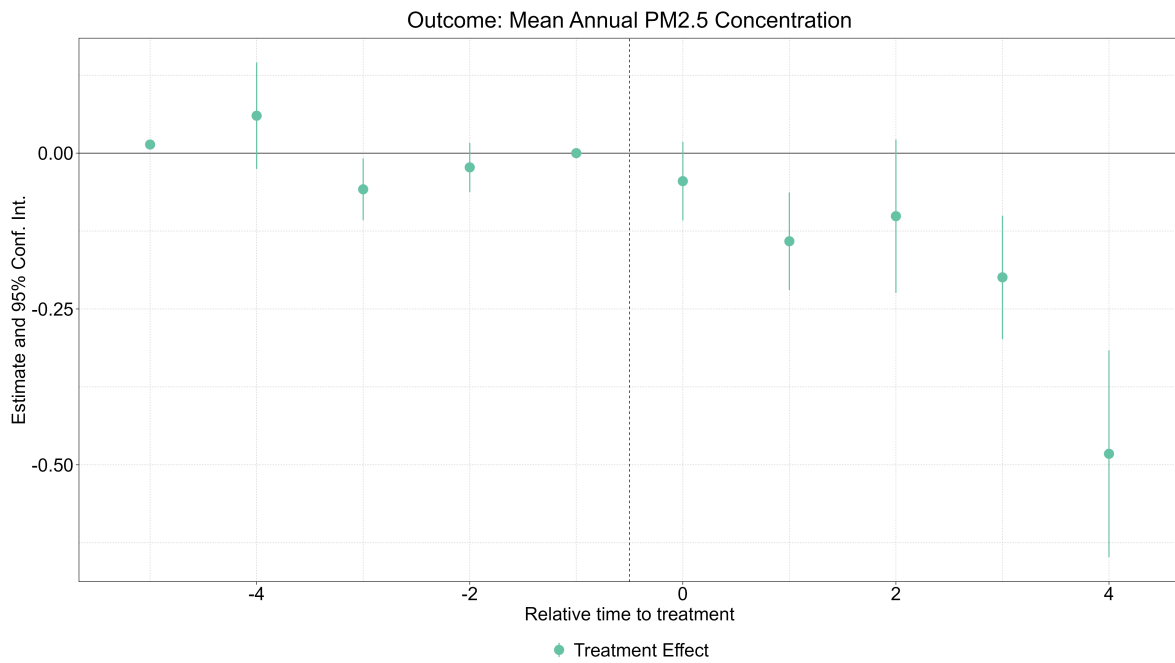
Note: The figure shows the average share of grid cells for a given within-district income percentile that is located within the direct vicinity of an operating IRD site. A grid cell is defined as being within the direct vicinity of a plant if the plant is located within the focal or one of the adjacent grid cells. Income percentiles are computed as rolling within-district percentiles for every year. PM2.5 concentration is averaged across all years in the sample.

Figure A.7: Location of Facility Closures in Germany



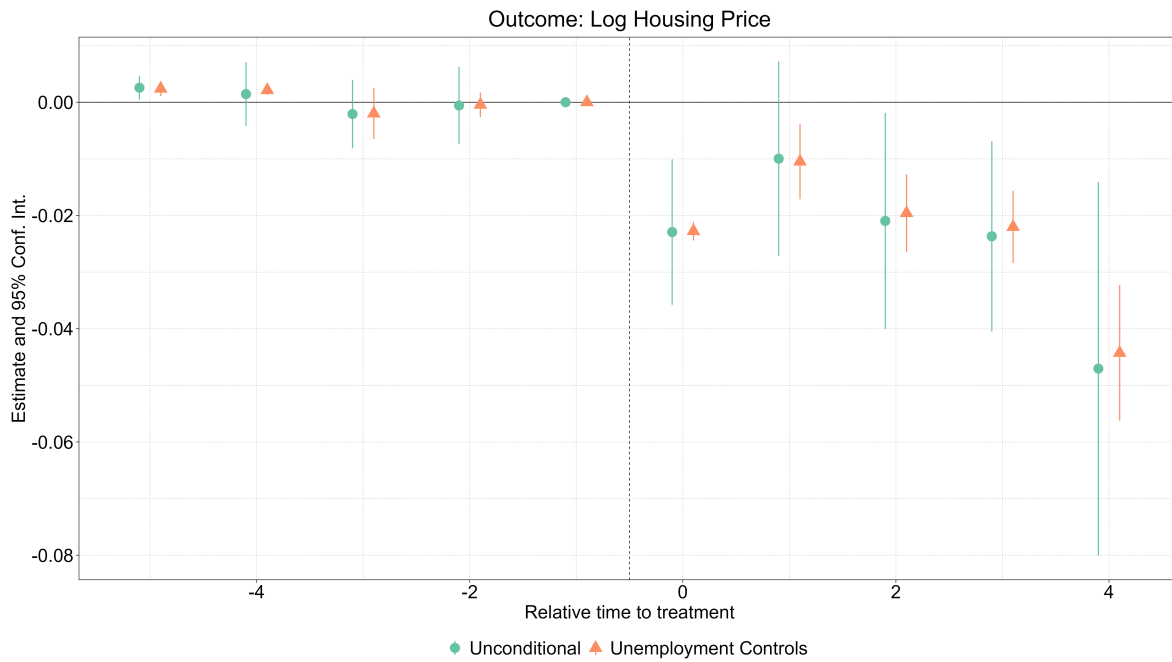
Note: The map shows the spatial distribution of plant closures in Germany across all years of the sample. The displayed radii are slightly larger than the ones used to define treatment in the empirical analysis to improve visual clarity.

Figure A.8: Effect of Facility Closures on Ambient PM_{2.5} Concentration



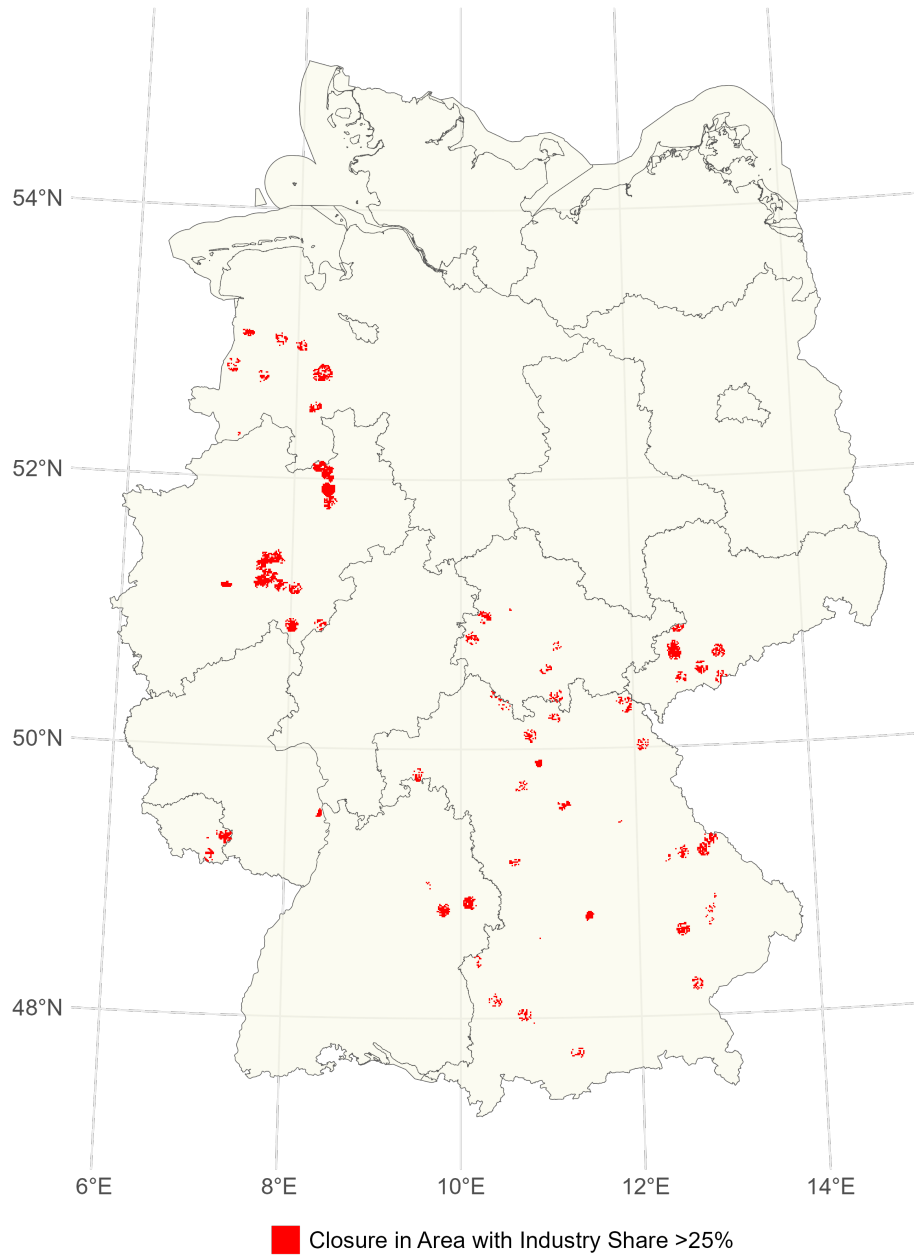
Note: The figure shows point estimates and 95% confidence intervals for θ_s in Equation 2. The outcome variable is mean annual ambient PM_{2.5} concentration at the grid cell level. The regression includes for mean annual temperature and precipitation at the grid cell level. The sample consists of all grid cells within a 5km radius around plants that close down during the sample period. Standard errors are clustered by *Bundesland*. All estimates are weighted by grid cell population.

Figure A.9: Effect of Facility Closures on Housing Price per sqm (in logs)



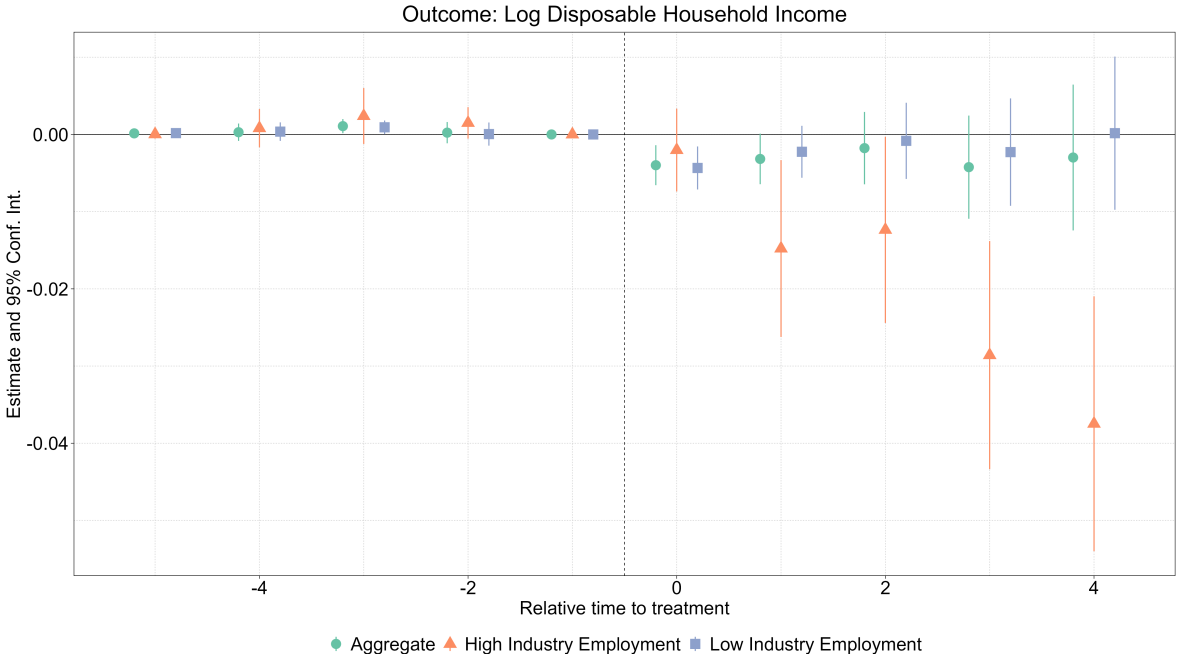
Note: The figure shows point estimates and 95% confidence intervals for θ_s in Equation 2. The dots represent the same estimates as in Figure 3, the triangles represent estimates while controlling for grid cell unemployment rates. The sample consists of all grid cells within a 5km radius around plants that close down during the sample period. Standard errors are clustered by *Bundesland*. All estimates are weighted by grid cell population.

Figure A.10: Spatial Distribution of Places Experiencing Significant Income Losses



Note: The map shows all places in Germany that experience a facility shutdown and are located within a district where the industrial employment share is at least 25%. These places correspond to the subsample used to estimate the effects in Figure 4.

Figure A.11: Effect of facility closures on mean disposable household income in surrounding grid cells with unemployment controls



Note: The figure shows point estimates and 95% confidence intervals for θ_s in Equation 2. The outcome variable is log disposable household income per adult at the grid cell level. The figure represents the same estimates as in Figure 4, but controlling for unemployment. The sample consists of all grid cells within a 5km radius around plants that close down during the sample period. Standard errors are clustered by *Bundesland*. All estimates are weighted by grid cell population.

A.3 Tables

Table A.1: Relative PM2.5 Exposure by Income Decile
Regression Results from Equation 1

Dependent Variable:	PM2.5			
	Grid Cell		Municipality	
Model:	(1)	(2)	(3)	(4)
Income Decile 2	-0.1483*** (0.0237)	-0.1096*** (0.0093)	-0.2122*** (0.0183)	-0.0026 (0.0075)
Income Decile 3	-0.3451*** (0.0325)	-0.1445*** (0.0126)	-0.2548*** (0.0220)	-0.0323*** (0.0094)
Income Decile 4	-0.4757*** (0.0369)	-0.1500*** (0.0140)	-0.2460*** (0.0243)	-0.0535*** (0.0110)
Income Decile 5	-0.4872*** (0.0397)	-0.1470*** (0.0150)	-0.2102*** (0.0260)	-0.0600*** (0.0121)
Income Decile 6	-0.4628*** (0.0414)	-0.1489*** (0.0157)	-0.1458*** (0.0272)	-0.0644*** (0.0134)
Income Decile 7	-0.4084*** (0.0427)	-0.1494*** (0.0167)	-0.0748*** (0.0286)	-0.0558*** (0.0147)
Income Decile 8	-0.3561*** (0.0435)	-0.1516*** (0.0181)	-0.0190 (0.0299)	-0.0562*** (0.0164)
Income Decile 9	-0.3207*** (0.0455)	-0.1597*** (0.0204)	0.0190 (0.0320)	-0.0605*** (0.0188)
Income Decile 10	-0.3126*** (0.0554)	-0.1631*** (0.0246)	0.0702** (0.0353)	-0.0372* (0.0221)
Share Foreign Born	-0.0029 (0.0030)	-0.0013*** (0.0004)	-0.0028 (0.0022)	-0.0124*** (0.0012)
Precipitation	-0.0166*** (0.0025)	0.0242*** (0.0006)	-0.0291*** (0.0012)	0.0282*** (0.0004)
Temperature	0.3322*** (0.0294)	-0.4628*** (0.0255)	0.0380** (0.0193)	0.4392*** (0.0198)
<i>Fixed-effects</i>				
Year	Yes	Yes	Yes	Yes
Grid Cell		Yes		
Municipality				Yes
<i>Fit statistics</i>				
Observations	2,078,131	2,078,131	139,710	139,710
R ²	0.71889	0.94622	0.76443	0.94518
Within R ²	0.08603	0.05499	0.09044	0.04103

Standard errors clustered by Municipality

*Signif. Codes: ***: 0.01, **: 0.05, *: 0.1*

Table A.2: Income Effects of Plant Closures by Industrial Employment Share

Dependent Variable: Mean Disposable Household Income		
Model:	Industry Share	
	$\leq 25\%$	$> 25\%$
<i>Relative Time</i>		
t - 5	0.0115* (0.0065)	0.0049 (0.0071)
t - 4	-0.0032 (0.0176)	0.0107 (0.0367)
t - 3	0.0447*** (0.0157)	0.0577 (0.0563)
t - 2	-0.0097 (0.0252)	0.0304 (0.0287)
t	-0.1409*** (0.0482)	-0.0277 (0.0588)
t + 1	-0.0672 (0.0452)	-0.3811** (0.1650)
t + 2	-0.0663 (0.0652)	-0.3641** (0.1691)
t + 3	-0.1168 (0.0998)	-0.8009*** (0.2139)
t + 4	-0.0731 (0.1539)	-0.9308*** (0.2161)
<i>Baseline Income</i>		
Estimation Sample	27.42	27.48
Full Sample	27.57	28.13
<i>Fit statistics</i>		
Observations	187,882	34,801
R ²	0.00154	0.07952
Adjusted R ²	0.00150	0.07931

Custom standard-errors in parentheses
*Signif. Codes: ***: 0.01, **: 0.05, *: 0.1*

Table A.3: Effect of Facility Closures on All Outcomes for Full Estimation Sample
Regression Output for Equation 2 on listed outcomes

Dependent Variables: Model:	PM2.5 (1)	Log Income (2)	Unemployment (3)	Log Housing Pr (4)	Log Amenities (5)
t - 5	0.0138*** (0.0040)	0.0003* (0.0002)	-0.0168*** (0.0040)	0.0026** (0.0011)	0.0004 (0.0003)
t - 4	0.0600 (0.0435)	-0.0004 (0.0006)	0.0556** (0.0256)	0.0014 (0.0029)	0.0016 (0.0010)
t - 3	-0.0580** (0.0253)	0.0011** (0.0005)	0.0012 (0.0180)	-0.0021 (0.0031)	-0.0016 (0.0010)
t - 2	-0.0228 (0.0201)	8.39×10^{-5} (0.0007)	0.0126 (0.0159)	-0.0006 (0.0035)	6.38×10^{-5} (0.0015)
t	-0.0449 (0.0322)	-0.0043*** (0.0015)	0.0289 (0.0490)	-0.0229*** (0.0065)	-0.0029 (0.0024)
t + 1	-0.1414*** (0.0399)	-0.0029* (0.0016)	-0.0194 (0.0507)	-0.0100 (0.0087)	-0.0017 (0.0029)
t + 2	-0.1011 (0.0628)	-0.0036 (0.0023)	0.1531* (0.0911)	-0.0210** (0.0097)	-0.0054 (0.0038)
t + 3	-0.1993*** (0.0505)	-0.0064** (0.0030)	0.1839* (0.0955)	-0.0237*** (0.0086)	-0.0027 (0.0031)
t + 4	-0.4824*** (0.0846)	-0.0068 (0.0050)	0.3228** (0.1451)	-0.0471*** (0.0168)	-0.0138** (0.0062)
Mean (SD) at t-1	11.77 (1.64)	3.30 (0.17)	6.97 (4.04)	7.77 (0.71)	–
Weather Controls	Yes	No	No	No	No
All models estimated with grid cell and bundesland \times year FE					
<i>Fit statistics</i>					
Observations	223,801	224,152	224,152	101,168	101,168
R ²	0.04098	0.00249	0.00640	0.00264	0.00116
Adjusted R ²	0.04095	0.00245	0.00636	0.00256	0.00108

Standard errors clustered by Municipality

*Signif. Codes: ***: 0.01, **: 0.05, *: 0.1*